Institute of Veterinary Biochemistry and Molecular Biology
der Vetsuisse-Fakultät Universität Zürich

Direktor: Prof. Dr. Ulrich Hübscher

Arbeit unter wissenschaftlicher Betreuung von
Dr. Manuel Stucki

Investigations on phosphospecific interactions in the DNA damage response

Inaugural-Dissertation

zur Erlangung der Doktorwürde der
Vetsuisse-Fakultät Universität Zürich

vorgelegt von

Mario-Emanuel Bonalli

Tierarzt
von Zürich, Schweiz

genehmigt auf Antrag von

Prof. Dr. Ulrich Hübscher, Referent

PD Dr. Thomas Riediger, Korreferent

Zürich 2009

Index of contents

1.1 Summary

Double strand breaks (DSBs) are one of the most dangerous forms of DNA damage. A globular cellular response is activated upon induction of DSBs. Mediator of DNA damage checkpoint 1 (MDC1) is one of those proteins involved in the DNA damage response (DDR) that contains an N-terminal forkhead associated (FHA) domain and a tandem BRCA1 C-terminal (BRCT) domain. MDC1 is recruited to sites of DNA damage upon phosphorylation of variant histone 2A (H2AX) by the kinase ataxia telangiectasia mutated (ATM).

In order to identify the amino acids that are targeted by ATM, we took a candidate approach and mutated a Threonine residue at the N-terminus of MDC1 to Alanin. We then performed an ATM kinase assay using radioactive ATP in order to check whether the T4A mutant fragment was still phosphorylated by ATM. Results of this study clearly revealed that ATM phosphorylates Thr 4 in MDC1 in vitro. We suggest that Thr4 is the major ATM phosphorylation site within the N-terminus of MDC1.

In a second part of this work, we sought to develop a proteomics approach to identify novel components of the DDR. We set up a tandem affinity purification (TAP) system using the BRCA1-BRCT domains fused to enhanced yellow fluorescent protein (EYFP) and triple-tagged at the C-terminus by a Streptavidin-binding peptide (Strep-tag II) a Flag-tag and an S-tag. As the Strep-tag II did not efficiently bind to Streptavidin, the performance of a TAP was not successful.

1.2 Zusammenfassung

DNS Doppelstrangbrüche (DSB) gehören zu den gefährlichsten DNS Schäden und führen zu einer weitgreifenden zellulären Antwort. Mediator of DNA damage checkpoint 1 (MDC1) ist ein Protein dieser DNA damage response (DDR) und besitzt eine N-terminale FHA als auch eine C-terminale tandem BRCT Domäne. MDC1 wird als Folge der Phosphorylierung von variant Histone 2A (H2AX) durch die Kinase Ataxia Telangiectasia mutated (ATM) zum Ort eines DNS Schadens rekrutiert.

Um die von ATM phosphorylierte Aminosäure zu identifizieren, wurde Thr4 als potentieller Kandidat zu Ala ummutiert. Mit radioaktivem ATP wurde ein ATM-Kinase Assay durchgeführt um herauszufinden ob das T4A mutierte Fragment immer noch phosphoryliert wird. Die Ergebnisse zeigten, dass T4A von ATM *in vitro* phosphoryliert wird. Folglich ist T4 die einzige ATM Phosphorylierungsstelle am N-Terminus von MDC1.

In einem zweiten Teil entschieden wir uns ein Proteomicsverfahren zu etablieren um neue Komponenten der DDR zu identifizieren. Wir entwickelten eine Tandem Affinity Purification (TAP), bestehend aus der BRCA1 BRCT Domäne verbunden mit dem enhanced yellow fluorescent protein (EYFP) und einem Trippel-tag am C-Terminus gebildet von einem Streptavidin-bindenden Peptid (Strep-tag II), einem Flag-tag und einem S-tag. Da der Strep-tag II nicht effizient von Streptavidin gebunden wurde, blieb die Durchführung der TAP erfolglos.

2. Introduction

The human genome exists of 3 billion base pairs and forms a sensitive unity in combination with various proteins localized in the cell nucleus. The maintenance of the genetic code is of prime importance; small alterations can cause serious consequences. A single mutation can already lead to severe developmental disorder or cancer formation. Our genome is in permanent danger from unavoidable DNA-damaging agents like ultraviolet light, ionizing radiation or genotoxic agents, which induce such mutations if left unrepaired. However, not only environment endangers genomic integrity but also byproducts of our normal cell cycle cause numerous forms of damage. Attention is focused on reactive oxygen species (ROS), which accumulate from oxygen respiration or as products of lipid peroxydation (Hoeijmakers et al., 2001).

In general, cancer formation is promoted when critical genes are mutated (Vogelstein et al., 2004). There are two major factors that affect mutation rate; exposure to carcinogens as already mentioned but also efficiency of cellular pathways that process DNA damage (Paz-Elizur et al., 2006). This process comprises the faultless execution of genome surveillance pathways that detect, signal and repair DNA damage and thereby coordinate cell cycle progression to ensure correct DNA replication and gene expression. Mutations or chromosomal aberrations caused by unrepaired or incorrectly repaired DNA damage can also lead to cell apoptosis, immunodeficiency, premature aging and neurodegeneration (Stucki, Clapperton et al., 2005).

DNA can be damaged in various forms. However, DNA double strand breaks (DSBs) are of special interest because of their enormous reparation investigations resulting in a high mutation risk. Thus, DSBs represent one of the most difficult kinds of damage to be repaired accurately. A double strand break occurs when both strands of the DNA double helix rupture and complementary overhangs cannot keep DNA ends juxtaposed just by base pairing, so that they dissociate from each other. DSBs not only arise from ionizing radiation or radiomimetic chemicals but also from mechanic stress on chromosomes, as products of collapsed replication forks or even from a physiological event during V(D)J recombination in developing B- and T-lymphocytes to achieve antigen binding diversity (Jackson 2002).

2.1. DNA Double Strand Breaks

2.1.1. DSB repair mechanisms

Due to their importance for all forms of life, DSB repair mechanisms are highly conserved through out evolution and can be found in phages, bacteria, yeast and higher eukaryotes (Cromie et al., 2001). There are two main repair pathways for DSBs; homologues recombination (HR) and non-homologues end joining (NHEJ). These two pathways differ in their occurrence during cell cycle. In mammalian cells the NHEJ repair mechanism prevails particularly in G0- and G1- phase, whereas HR predominates mainly in S- and G2-phase when the undamaged sister chromatid can be used as a template (Shrivastav et al., 2008).

2.1.2. Non-homologous end joining

Although NHEJ works not as accurately as HR it is the predominant repair mechanism in higher eukaryotes. When no sister chromatid is present free DNA ends are directly joined often by adding or deleting nucleotides (Budman et al., 2005). In mammalian cells NHEJ is used to repair DNA DSBs and to join gene segments during V(D)J-recombination in developing lymphocytes. The DNA dependent protein kinase (DNA-PK) plays a central role in NHEJ and is activated upon association with DNA. DNA-PK is a serine-threonine kinase consisting of a DNA binding subunit and a catalytic component (Smith and Jackson et al., 1999). The Ku protein representing the DNA binding subunit is a heterodimer of 70 and 86 kDa that binds to DNA ends, nicks and structures containing a transition fork between double-stranded DNA and two single strands. The Ku protein makes no contacts with DNA bases and only few with the sugar-phosphate backbone so that DNA end interactions are structure and sequence-independent. The crystal structure of the Ku70-Ku80 complex reveals a central domain forming a double ring that encircles the DNA molecule (Riha et al., 2006). Ku and the DNA-PK catalytic subunit (DNA-PKcs) show only weak association in the absence of free DNA ends. However, when the Ku heterodimer binds to DNA ends, the Ku80 subunit changes its conformation and a 12-amino acid sequence from the C terminus becomes exposed. This sequence specifically binds and

recruits the 465kDa DNA-PKcs to the DNA end. DNA-PKcs contains a separate DNA binding domain that binds DNA ends with much lower affinity and specificity as compared to Ku (Martensson et al., 2002). Sequence analysis of the catalytic domains revealed DNA-PKcs to be a member of the phosphatidylinositol 3-kinase-like family (PIKK) that also includes ATM (ataxia telangiectasia mutated) and ATR (ATM related) (Hartley et al., 1995). Further studies have shown that a single stranded DNA end derived from a DSB is essential for DNA-PKcs activation (Hammarsten et al., 2000). DNA-PKcs also recruits and forms a complex with Artemis. DNA-Pkcs activates Artemis by phosphorylation and shows endonuclease hairpin opening activity (Ma et al., 2002), (Riha et al., 2006). Lack or mutations of DNA-PK subunits can lead to radio hypersensitivity or severe combined immunodeficiency.

Although there are four DNA ligases expressed in mammalian cells encoded by three different genes, only Ligase 4 (Lig4) is involved in NHEJ. Lig 4 forms a 1:2 complex with the DNA repair factor XRCC4, which is necessary for ligase activity. The Lig4/XRCC4 complex has a unique single-strand ligation activity that permits joining of only one strand with the opposite strand (Grawunder et al., 1998), (Riha et al., 2006). If DNA ends are compatible the ligation occurs immediately. If not, Artemis processes DNA ends until the Lig4/XRCC4 complex is capable to ligate them. DNA ends can also be resected by the MRN-complex, which harbors exo- and endonuclease activity as well as helicase and adenylat kinase activity. Finally, polymerases terminate NHEJ by filling the gaps, before Lig4/XRCC4 completes the joining reaction (Ma 2002) (see Figure 1).

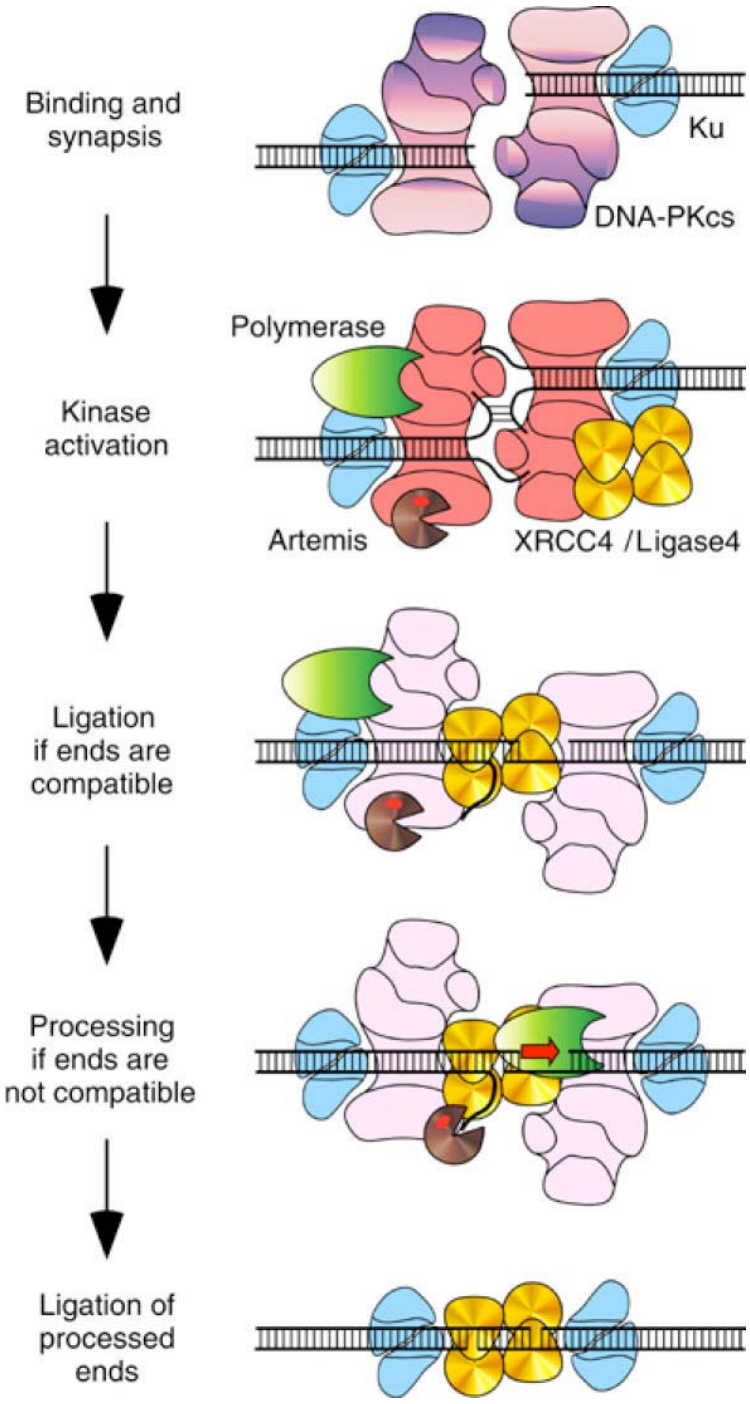

Figure 1; Non-homologous end joining mechanism in DNA double-strand break repair

(Adapted from Budman et al., EMBO journal, 2005)

Ku heterodimer binds to DSB and targets DNA-PKcs to DNA. Together, Ku and DNA-PKcs form the catalytically active DNA-PK holoenzyme. Then, Ku recruits ligase 4 along with XRCC1 and DNA-PK-dependent phosphorylation of XRCC1 influences its activity. Ligation process occurs immediately, if the DNA ends are compatible. Otherwise polymerase and nuclease activities process DNA ends into compatible substrates so that ligase 4/XRCC1 complex can complete the joining process.

2.2. Cellular responses to DNA double-strand breaks

The induction of DSBs not only leads to activation of the repair pathways but also to globular cellular respone that inclutes regulation of cell cycle transitions, transcriptional activation and apoptosis. The cellular response to DSBs starts with the detection of the DNA lesion by sensory proteins, which trigger the activation of kinase-dependent signaling cascades. This so called DNA damage response (DDR) is a classical signal-transduction pathway consisting of sensors, transducers and effectors. In order for a single DSB to induce a cell cycle arrest, the initial signal must be amplified and diversified to a series of downstream effectors that control diverse cellular functions (Khanna et al., 2001).

A conserved signaling component with a central role in cellular response to DSBs is ATM (ataxia telangiectasia mutated). The physiological importance of ATM is demonstrated in patients suffering from ataxia telangiectasia. Patients carrying two mutated ATM alleles exhibit progressive cerebellar ataxia, immune deficiencies, gonadal atrophy, oculocutaneous telangiectasias, radiation sensitivity, premature ageing and increased risk of cancers, particularly lymphomas (Bakkenist et al., 2003). The ATM gene encodes a 370-kDa protein that belongs to the phosphatidylinositol 3-kinase-like (PIKK) family. In undamaged cells ATM exists as a homodimer, hiding the 350 amino acid kinase domain at the carboxy terminus. ATM gets recruited to DNA DSBs through the MRN complex, which consists of MRE11, RAD50 and NBS1 (Stucki et al., 2004), (Falck et al., 2005). MRN is among the first proteins that accumulate at sites of DSB in eukaryotic cells. NBS1 containing a FHA and BRCT domains and acts as a crucial mediator and adaptor in the DDR. Mutations in the NBS1 gene lead to Nijmegen breakage syndrome (NBS) in humans, and cells derived from NBS patients display a DSB repair defect and DNA damage signaling deficiencies. MRE11 is a structure-specific nuclease involved in DNA-end processing, while RAD50 displays ATPase and adenylate kinase activity (D'Amours et al., 2002), (Stracker et al., 2004), (Jazayeri et al., 2006), (Costanzo et al., 2004). Activation of the MRN complex leads to ATM auto-phosphorylation on multiple residues and the ATM dimers dissociate to active monomers which phosphorylate a variety of target proteins such as checkpoint kinase 2 (CHK2), mediator of DNA damage checkpoint 1 (MDC1), p53 binding protein 1 (53BP1), breast cancer

susceptibility protein (BRCA1) and histone 2A variant (H2AX). These phosphorylation events do not only target downstream factors regulating the repair pathways, they can also lead to transient or permanent cell cycle arrest if the damage persists, or to programmed cell death when DNA damage is too extensive. Phosphorylation of H2AX on Ser139 by ATM at sites of DNA damage leads to recruitment of MDC1, an important mediator protein. MDC1 acts to amplify H2AX phosphorylation, possibly by recruiting ATM into the DSB-flanking chromatin compartment or by preventing H2AX dephosphorylation (Stucki et al., 2006). Our lab established a model proposing that MRN and MDC1 exist as a complex whereby MDC1 mediates the recruitment of MRN to γH2AX-containing chromatin (Spycher et al., 2008) (Kobayashi et al., 2002). MDC1 and phosphorylated H2AX allow the recruitment of many additional factors, that form the so-called DNA damage foci. One of those factors is 53BP1, a mediator that plays a role in CHK2 and p53 activation (Harper et al., 2007). How 53BP1 gets recruited is still not entirely clear. MDC1 recruits Ubc13-Rnf8, an E3 ubiquitin ligase complex that ubiquitinylates H2A and H2AX and possibly other factors at sites of DSBs. 53BP1 and BRCA1 recruitment seem to depend on this poly-ubiquitination (Huen et al., 2007), (Kolas et al., 2007), (Mailand et al., 2007), (Wang et al., 2007). BRCA1 that is also recruited into DNA damage foci appears to have also a direct or indirect role in transcriptional activation as a component of the RNA polymerase II holoenzyme (Monterio et al., 1996), (Chapman et al., 1996). BRCA1 contains, just like RNF8 a RING-finger domain and was observed to have E3 ubiquitin ligase activity that might be relevant in signal transduction (Baer et al., 2002). Recent studies revealed BRCA1 itself, H2A and H2AX and p53 as potential candidate substrates (Chen et al., 2002), (Vandenberg et al., 2003), (Billack et al., 2004).

Effector proteins are either direct targets of ATM or are phosphorylated by the two checkpoint transducer kinases CHK1 and CHK2. The tumor suppressor p53 is one of the major effector proteins and is known to be mutated in many cancer cells. Once activated, it acts as a transcription factor regulating for example the expression of p21, a Cdk inhibitor protein responsible for G1 cell cycle arrest. Further on, the accumulation of p53 provokes apoptosis by activating the caspase-signaling cascade. In addition, Cdc25 phosphatase is another important effector of the DDR that controls cell cycle progression through regulation of cycline dependent kinases (CDKs) (Zhou 2000) (see Figure 2).

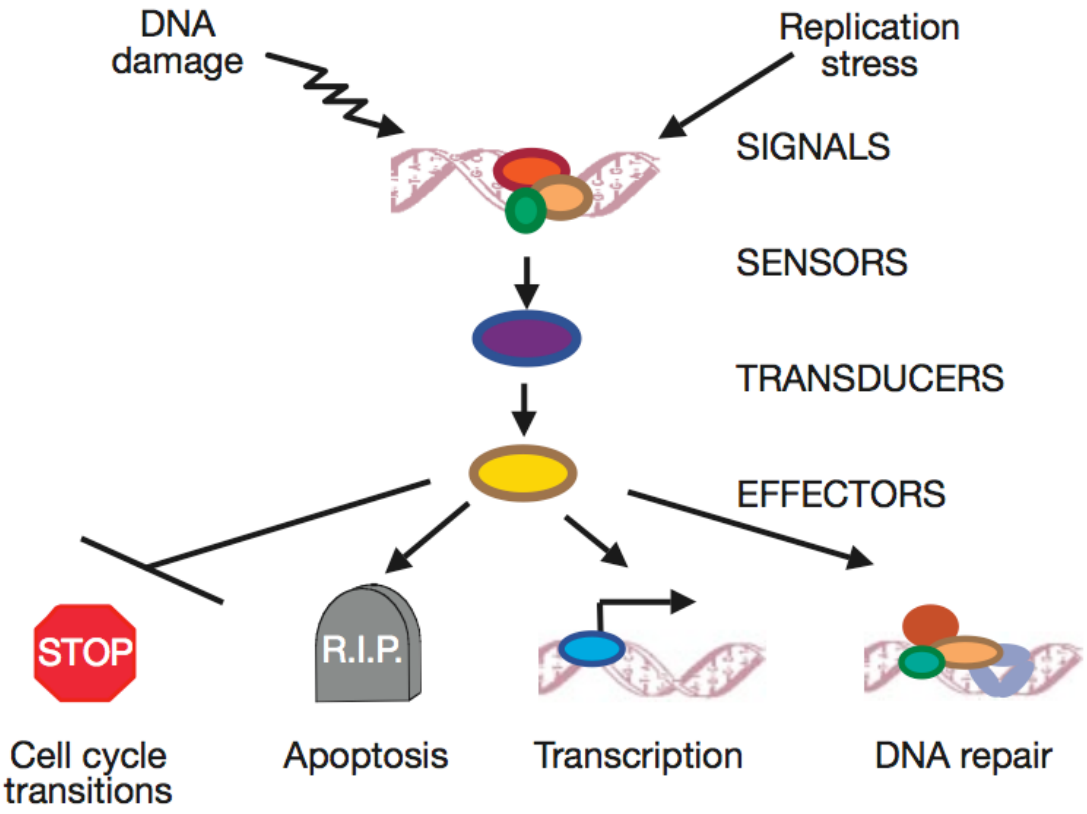

Figure 2; Overview of the DNA damage response signal-transduction pathway

(Adapted from Zhou and Elledge, Nature, 2000)

Exposure of DNA to various agents lead to DNA damages that are recognized by multiple sensor proteins. This results in the activation of proximal kinases that trigger the activation of transducer proteins. Protein kinase cascades amplify and diversify the DNA damage signal and activate multiple downstream effector proteins that regulate different aspects of cellular function. Adaptor proteins influence coordination of DNA repair and are also important for signal amplification.

2.3. MDC1

A key regulator of ionizing radiation induced foci (IRIF) formation in mammalian cells is histone variant H2AX, a component of the nucleosome core structure. H2AX comprises 10-15% of total cellular H2A in higher organisms and becomes rapidly phosphorylated on a C-terminal Ser residue (Ser139) in response to DNA damage. This phosphorylation is PIKK-dependent. In the past few years, research has focused on finding interaction partners for phosphorylated H2AX (termed γH2AX). One of those discovered proteins that recognize and interact with phosphorylated H2AX is Mediator of DNA damage checkpoint 1 (MDC1). Interestingly, SDS-PAGE analysis revealed MDC1 to exist in three isoforms probably due to alternative splicing. MDC1 contains two phosphorylation-specific interaction domains: a tandem breast cancer associated carboxy-terminal (BRCT) domain at the C-terminus and a forkhead associated (FHA) domain at its N-terminus (see Figure 3). Additionally, a large S/TQ cluster domain can be found encompassing the N-terminal part of the protein. S/TQ cluster domains (also present in BRCA1 and ChK2) are phosphorylated by ATM in response to DNA damage. Further domain analysis of MDC1 revealed a large central proline/serine/threonine-rich (PST) repeat domain that has no significant homology to any other protein (Stewart et al., 2003). MDC1 is not only claimed to be a mediator of damage checkpoint but also a mediator of damage repair since cells deficient in MDC1 display defects in DSB repair by HR (Xie et al., 2007) and NHEJ (Lou et al., 2004). MDC1 shows dispersed localization in nuclei of undamaged cells whereas γ-irradiation leads to accumulation at sites of DSBs that appears in fluorescence microscopy as bright nuclear foci that colocalize with H2AX foci. Cells lacking MDC1 are sensitive to ionizing radiation, disabled in foci formation and fail to activate the intra-S phase and G2/M phase cell cycle checkpoints properly after exposure to ionizing radiation, indicating that it is an important player in the cellular response to DSBs.

Biochemical and structural analysis recently revealed that the tandem BRCT domain of MDC1 directly interacts with phosphorylated Ser139 residue of H2AX in a tight and highly specific manner (Stucki et al., 2005). This interaction is essential for MDC1's relocalization in IRIF upon irradiation and abrogation of this interaction

triggers similar effects as loss of MDC1, indicating that it is functionally relevant. In addition to the C-terminal BRCT domains, MDC1 also features an FHA domain at its N-terminus. The MDC1 FHA domain recognizes phosphorylated threonine residues and recent study suggested MDC1 to play an essential role in the signal transduction of the ATM-p53 pathway that regulates apoptosis. In this study, it was reported that MDC1 associates with the ATM-phosphorylated protein kinase ChK2 through its FHA domain (Lou et al., 2003). Since a putative MDC1 FHA recognition sites has recently been discovered in MDC1 itself by our laboratory (Jungmichel et al. personal communication), further investigations were necessary to confirm that this putative FHA recognition site located at the N-terminus of MDC1 is indeed targeted by the ATM kinase (see results).

Figure 3; Schematic overview of MDC1 domains

MDC1 consists of 2089 amino acids and harbors several domains involved in protein interactions. The N-terminal FHA domain plays a crucial role in recognition of phosphorylated serine/threonine motifs. It was also shown that MDC1 interacts via its BRCT domain with phosphorylated H2AX at Ser139.

2.4. BRCA1

The tumor suppressor gene encoding breast cancer 1 susceptibility protein (BRCA1) was among the first discovered genes bearing a hereditary predisposition for the development of breast and ovarian cancer. The BRCA1 gene is mutated in 8.5% of all breast cancer cases and over 450 mutations have been identified (Hemminki et al., 2004). Whereas the lifetime risk of developing breast (45-87%) or ovarian (37-66%) cancer with inherited BRCA1 mutations is high, the risk of cancer in other tissues is small. Hormonal interference between BRCA1 and estrogen is a possible explanation for this tissue specificity as BRCA1 is reported to bind and inhibit the action of the estrogen-receptor. The importance of BRCA1 in the DDR is revealed by the fact that BRCA1 deficiency is compromising homologues recombination, transcription-coupled repair, micro-homology end joining and NHEJ (Billack et al., 2005).

BRCA1 consists of an amino terminal RING (really interesting new gene) -finger domain, a centrally located nuclear localization signal (NLS) and a C-terminal tandem BRCT domain (see Figure 4). Initially, the presence of these domains led to the hypothesis that BRCA1 acts as an acidic transcription factor. In fact, BRCA1 was later found to be a component of the RNA polymerase II holoenzyme. However, BRCA1 seems to be implicated in many aspects of transcription, although it is unlikely that it acts as a classical transcription activator but rather as a co-activator. It was also observed that the RING finger, an E3 ubuquitin ligase domain rather functions here as a protein-protein interaction motif and mediates the binding of BRCA1 to its partner BARD1. BARD1 also contains a BRCT and a RING finger domain, and both proteins dimerize via their RING finger domains. The biochemical function of this double RING domain was revealed to serve as an efficient E3 ubiquitin ligase with strong preference for polyubiquitination. Although polyubiquitination was associated with targeting proteins for degradation, it also seems to participate in the DDR as a mediator or adaptor (Scully et al., 2004), (Billack et al., 2005). Several other proteins bind to the C-terminal BRCT domains of BRCA1. One of those BRCT interacting proteins is CTBP interacting protein (CtIP) that as the name implies bind CTBP, a transcriptional co-repressor. This gives further evidence that BRCA1 acts in transcriptional regulation eventually by targeting the CtBP pathway of transcriptional repression. In addition, a stable BRCA1-CtIP

complex is required for BRCA1-mediated tumor suppression (Yu et al., 1998). Another BRCA1 BRCT interacting protein is BACH1 (BRCA1 associated carboxyl-terminal helicase 1), a member of the DEAH helicase family (also known as BRIP or FancJ). A solid interaction between BRCA1 and BACH1 is required for a proper execution of DSB repair. Mutations that lead to abrogation of the interaction increase the risk of cancer development (Cantor et al., 2001). Recent studies found that the BRCA1 BRCT domain also interacts with RAP80, a ubiquitin-binding protein (Sobhian et al., 2007). Fluorescent microscope analysis revealed BRCA1 also to co-localize and form a complex during homologues recombination and meiotic prophase with RAD51 recombinase, an important component of the HR pathway that binds single-stranded DNA (Scully et al., 2004). In summary, through its C-terminal BRCT domains, BRCA1 may serve as an adaptor in phosphorylation-dependent protein-protein interaction networks that are regulated by various kinases either in a cell cycle-dependent manner or in response to DNA damage.

The wide operating range of BRCA1 highlighted by the broad band of interaction partners demonstrates its fundamental role in the DNA damage response and its importance as a tumor suppressor.

Figure 4; Schematic overview of BRCA1 domains

BRCA1 consists of 1863 amino acids and harbors an N-terminal RING finger domain a central located NLS and a C-terminal BRCT domain. BRCA1 forms a heterodimer with BARD1 through its RING finger domain and the BRCT domain was also shown to interact with BACH1, CtIP and RAP80 in a phosphorylation dependent manner.

2.5. The FHA domain

Each cell represents a dynamic complex that grows, divides differentiates and reacts to environmental influence. Communication within the cell is absolutely necessary therefore a highly conserved signal transduction system connects and regulates all kinds of pathways ensuring cell survival. Signaling protein modules are small independently folded units having a variety of functions. An important class of signaling modules are the protein-binding domains recognizing phosphorylated epitopes. This class of signaling modules comprises the SH2, PTB and WW domains, 14-3-3 proteins and the subject of this chapter, the forkhead associated (FHA) domain. The evolution of phosphopeptide-recognizing and -binding modules is not surprising as kinase-dependent singal transduction pathways play a major role in almost all aspects of eukaryotic cellular function.

The FHA domain was discovered in 1995 (Hofmann and Bucher et al., 1995) and is a modular phosphopeptide binding domain with a striking specificity for phosphothreonine (pT) –containing epitopes. So far, the FHA domain has been found in more than 700 different proteins in species ranging from prokaryotes to higher eukaryotes. The FHA domain is not only associated with intracellular signal transduction, but also with proteins involved in numerous processes including transcription, protein transport, DNA repair and protein degradation (Durocher and Jackson et al., 2002). The FHA domain received its name after it was found in forkhead transcription factors. Surprisingly, only five amino acids are identical in most FHA domains consisting of 80 to 120 amino acids (Hofmann and Bucher et al., 1995). Four of these conserved amino acids are required for phospho-epitope interactions. Even though FHA domains show little sequence homology they are all structurally organized into a β-sandwich of six-stranded and five-stranded β-sheets. Three contiguous loops connecting β-strands from the five-stranded β-sheet form the contact interface to phosphorylated interaction partners (see Figure 5). The five conserved loop residues are surrounded by residues that differ among FHA domains in order to yield binding specificity (Liang et al., 2008). However, the FHA binding specificity is additionally influenced by the amino acid residues surrounding the

phospho-acceptor. The residue, mostly at pT +3 position but other positions are also possible (Durocher et al., 2000).

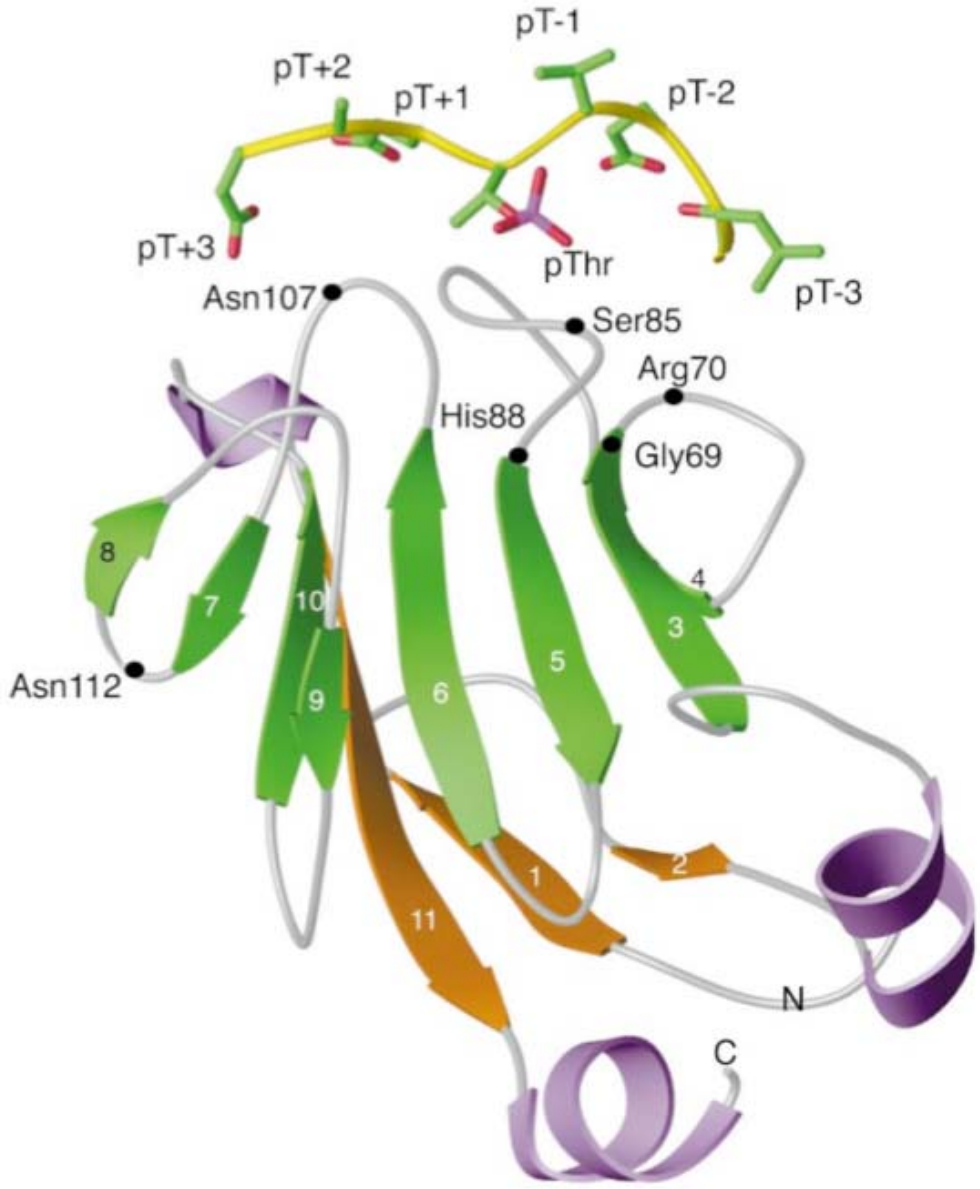

Figure 5; Crystal structure of the Rad 53 FHA domain

(Adapted from Durocher and Jackson, FEBS, 2002)

FHA domains are conserved phosphorylation dependent interaction modules comprising 80 to 120 amino acids. FHA domains are associated with intracellular signal transduction, transcription, protein transport, DNA repair and protein degradation. FHA domains are structurally organized as a six-stranded and five-stranded β-sheet, forming a β-sandwich.

2.6. The BRCT domain

The BRCT (BRCA1 C-terminal) domain, first identified in BRCA1, is an evolutionarily conserved module that exists in a large number of proteins from prokaryotes to eukaryotes. BRCT domains are predominantly found in proteins involved in DNA damage checkpoint, recombination events and DNA repair (Koonin et al., 1996), (Bork et al., 1997), (Callebaut and Mornon et al., 1997). Sequence analysis revealed the presence of 50 copies of the BRCT domain in 23 different proteins, including 53BP1, RAD9, XRCC1, RAD4, Ect2, REV1, Crb2, RAP1, terminal deoxynucleotidyltransferase (TdT) and three eukaryotic DNA ligases. BRCT domains are not always located at the C-termini of the proteins and despite they often appear in a tandem configuration (i.e. two consecutive BRCT domains in close proximity) they can also be found in a single copy or in multiple copies. BRCT domains usually comprise 80 to 100 amino acids and form an autonomous folded globular complex. X-ray crystallographic and nuclear magnetic resonance studies revealed a structure of three α-helices surrounding a central β-sheet composed of four parallel β-strands (see Figure 6). The structure is additionally stabilized by a salt-bridge and various hydrophobic interactions between α-helices and β-strands (Zhang et al., 1998).

It was recently demonstrated that tandem BRCT domains like FHA domains are phosphopeptide-binding motifs. In contrast to the FHA domain, it appears that tandem BRCT domains have a preference for phosphoserine and phosphothtronine residues. Thus, as SQ or TQ sequences are ATM phosphorylation consensus motifs, ATM is in many cases supposed to play a considerable role in the interplay with BRCT containing proteins (Manke et al., 2003), (Yu et al., 2003). The members of the BRCT domain-containing protein-family are usually large, multidomain proteins and besides BRCT domains, all of them, feature other functional domains involved in transcription, repair and replication or in other signal transduction events. Some of these proteins show enzymatic activity such as poly (ADP-ribose) polymerase (PARP), two DNA ligases and type X DNA polymerase whereas other members possess a RING-finger domain such as BRCA1, a FHA domain such as MDC1 or a DH domain such as ECT2 (Bork et a., 1997)

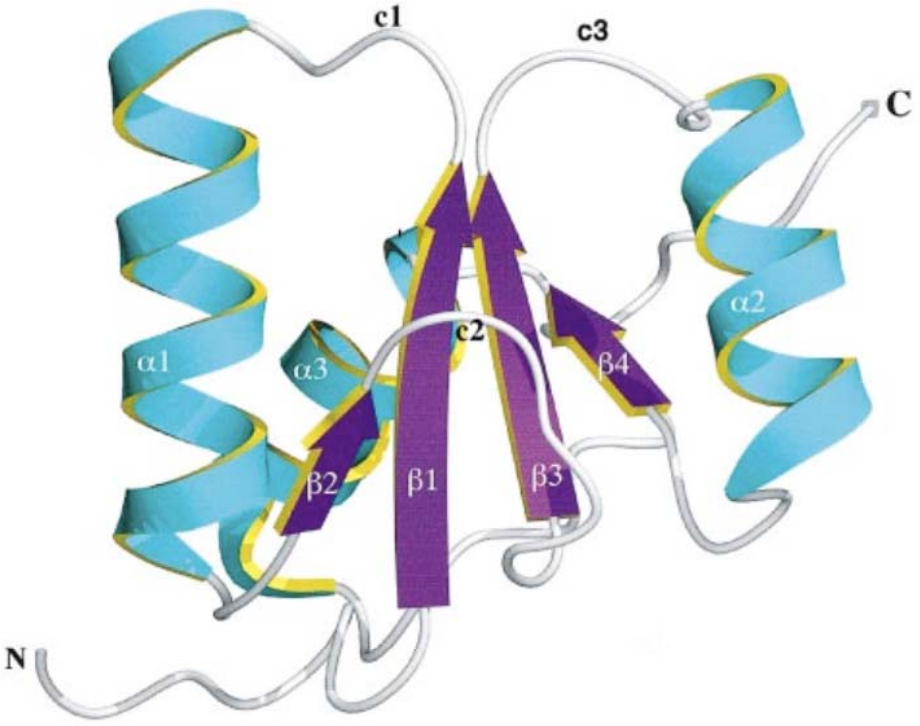

Figure 6; X-ray structure of the XRCC1 BRCT domain

(Adapted from Zhang and Morera, EMBO journal, 1998)

BRCT domains are evolutionarily conserved modules that occur alone, in tandems or in multiples and are predominantly found in proteins involved in cell cycle checkpoint, recombination or repair. They comprise 80 to 100 amino acids in which two to three α helices surround a central β-sheet comprising four parallel β-strands. BRCT domains are also phosphopeptid-binding motifs.

3. Materials and Methods

3.1. Materials

3.1.1. Antibodies

3.1.1.1. Primary Antibodies

Polyclonal mouse α-GFP (1:1000)	Abcam
Monoclonal mouse α-Flag M2 (1:1000)	Sigma
Monoclonal mouse α-Tubulin (1:2000)	Sigma
Polyclonal rabbit α-Flag (1:300)	Sigma
Rabbit α-Bach1 (1:4000)	a Gift from Josef Jiricny
Rabbit α-CtIP (1:4000)	a Gift from Alessandro Satori
TOM α-ATM antibody (1:400)	a Gift from Graeme Smith (KuDos Pharmaceutical)

3.1.1.2. Secondary Antibodies

Polyclonal ECL α-mouse horseradish peroxidase-linked sheep antibody (1:5000) GE Healthcare
Polyclonal ECL α-rabbit horseradish peroxidase-linked donkey antibody (1:5000) GE Healthcare

3.1.2. Antibiotics

Ampicilin (100mg/ml in dH2O)	Fluka Chemie AG
G418 sulfate, cell culture tested	Calbiochem®
Kanamycin	Fluka Chemie AG
Penicillin-Streptomycin (10’000 units/ml)	Invitrogen®

3.1.3. Bacteria strains

E.coli XL1blue
E.coli pLys S

3.1.4. Chemical reagents

Acetic Acid	Thommen Furler AG
Acrylamid-bis 40%	Serva®
Adenosintriphosphat	A kind gift from Manuel Stucki
Agarose	Promega Corporation®
Ammoniumperoxydisulfat	Fluka®
Bestatin	Bachem®
β-mercapto-ethanol	Fluka®
Bromphenol blue sodium	Sigma-Aldrich®
Calcium Chloride dihydrate	Fluka®
Citric Acid	Merck®
Coomassie Brilliant Blue R250	Fluka®
Copper Sulfate (CuSO4(5H2O))	Merck®
Disodiumhydrogenphosphat dihydrate	Fluka®
Dithiothritol	Fluka®
DMEM	Gibco®
DMSO	Fluka®
ECL (two solutions, mixed 1:1)	Amersham Biosciences®
Ethylendiamin-tetraacetic acid	Fluka®
Enlightening solution	Amersham Bioscience®
Ethanol	Merck®
Ethidium bromide solution 1% in H2O	Fluka®
Fetal calf serum (FCS)	Gibco®
αFlag M2 agarose	Sigma®
Folin-Ciocalteu's phenol reagent	Sigma®
Formaldehyde (HCHO)	Fluka®
γ32P-ATP	Hartmann Analytic®
Gluacal acetic acid	Fluka®
D(+) Glucose monohydrate	Fluka®
Glutathione	Sigma®
GSH-Sepharose	GE Healthcare®
Glycerol	Fluka®
Hydrochloride acid (HCl)	Merck®
HeLa nuclear extract	selfmade
4-(Hydrosyethyl) piperazine-1-ethanesulonic acid	Fluka®
Isopropanol	Sigma®
Isopropyl-β-D-thiogalactopyranoside	Biosynth®

KOH	
Leupeptin	Bachem®
Methanol	Merck®
Magnesium chloride (MgCl2)	Fluka®
MgSO4	Fluka®
NaHPO4	Fluka®
Nonidet P40	Fluka®
Pepstatin	Bachem®
Phenylmethansulfonylfluorid	Fluka®
Ponceau S	Sigma®
Protein A-Sepharose	GE Healthcare®
S-protein Agarose	Novagen®
Sodiumdodecylsulfat	Fluka®
Silver nitrate (AgNO3)	Fluka®
Sodium carbonate (Na2CO3)	Fluka®
Sodium chloride (NaCl)	Fluka®
Sodium citrate (Na3H5C6O2)	Fluka®
Sodium hydroxyde (NaOH)	Fluka®
Streptavidin agarose	Fluka®
Streptavidin dynabeads	Invitrogen®
N,N,N',N'-Tetramethylethylendiamin	Fluka®
Tris-(hydrosymethyl)-aminomethan	Biosolve®
Trypsin-EDTA (10x)	Invitrogen®
Tween 20	Fluka®
Xylen Cyanol	Merck®

1.5 Enzymes

BamHI	New England Biolabs®
CIP (calf intestine phosphatase)	New England Biolabs®
DpnI	Stratagene®
Expand High Fidelity Enzyme (100U/µl) Mix	Roche®
Pfu Turbo Polymerase	Stratagene®
Pfu Ultra Polymerase	Stratagene®
Pfu UltraII Polymerase	Stratagene®
T4-DNA-Ligase	Fermentas®
T4 PNK	New England Biolabs®
XbaI	New England Biolbas®
XhoI	New England Biolabs®

3.1.6. Human cell lines

293T
U2OS

3.1.7. Vectors

pEYFPnucTO human expression vector	BD Biosciences Clontech®
pGEX4T3 bacterial expression vector	GE Healthcare Bioscience®

3.2. Methods

3.2.1. DNA manipulations

3.2.1.1. Agarose Gelelectrophoresis

Digested plasmid DNA or PCR products were separated on a 1% agarose gel and visualized by ethidium bromide staining under a UV light source.

Buffers and Medias:
1x TAE buffer
6x Loading buffer
1kb Marker

Chemical Reagents:
Agarose
Ethidium bromide solution

Electrophoresis Kit:

Mini Sub DNA Cell	Bio-Rad® electrophoresis system
Power Pac 200 (at 80V)	Bio-Rad® power supplies
ChemiImager 5500	Alpha Innotech®

Gel preparations:

100ml	1xTAE buffer
1g	Agarose
4µl	Ethidium bromide solution

3.2.1.2. SDS-PAGE (SDS-polyacrylamid gel electrophoresis)

SDS-PAGE is a method to separate proteins according their molecular weight in a matrix by applying an electric field through the gel.

Buffers:
2x SDS loading buffer
1x Stacking-Gel buffer
2x Running-Gel buffer
1x Running buffer
Stain
Destain

Electrophoresis Kit:
Mini-Protean Tetra Electrophoresis System — Bio-Rad vertical electrophoresis system
Power Pac 200 (15min 80V, than 150V) — Bio-Rad power supplies

Gel preparation:

	6%	8%	10%		12%	15%	Stacking gel
2x Gel buffer	2.5ml	3ml	3ml	5ml	5ml	5ml	2.4ml
40% Acrylamid-bis (w/v)	0.75ml	1.2ml	1.5ml	2.5ml	3ml	3.75ml	0.375ml
dH2O	1.75ml	1.8ml	1.5ml	2.5ml	2ml		
APS 10%	50µl	60µl	60µl	100µl	100µl	100µl	30µl
TEMED	10µl	10µl	10µl	15µl	15µl	15µl	8µl

3.2.1.3. DNA-Digestion

DNA was digested for at least 2 hours at 37°C

Preparations:
5µl H2O
3µl DNA (1µg/µl)
1µl Buffer
0.5µl Restriction enzyme 1
0.5µl Restriction enzyme 2

After digestion, CIP phosphatase was added to the mix for 1 hour at 37°C to avoid self-ligation of the empty vector by phosphorylating 5'-ends.

1µl CIP — New England Biolabs

3.2.1.4. NucleoSpin® Gel-Extraction and PCR clean-up

The gel extraction and PCR clean-up was done according the Macherey-Nagel protocol (protocol at a glance, rev. 03) for NucleoSpin® Extract II by using mini spin columns with silica membrane technology.

Buffers and Medias:

NT binding buffer	Macherey-Nagel®
NT3 wash buffer	Macherey-Nagel®
NE elution buffer	Macherey-Nagel®

Material:

NucleoSpin® mini spin columns

3.2.1.5. Ligation Arrangements

Digested DNA fragments were ligated by T4 DNA ligase in the fridge at 4°C over night.

Preparations:

1µl	T4 DNA Ligase	Fermentas®
1µl	T4 Ligase Buffer	Fermentas®
4µl	Template	
4µl	Insert	

3.2.1.6. Mini Plasmid Preparation (Mini Prep)

To quantify and analyse recombinant plasmid DNA the following protocol was used:
The cell pellet from an overnight bacteria culture was collected by centrifugation (4000rpm for 10 minutes at 4°C) and resuspended in 250µl S1 buffer. When the pellet was well dissolved the S2 buffer was added for cell lysis and three minutes later the S3 buffer was added to precipitate proteins. The mix was centrifuged at 14000rpm for 15 minutes at 4°C. The supernatant was collected, mixed with 560µl isopropanol and incubated on ice for 10 minutes. After that, the mixture was centrifuged at 14000rpm for 30 minutes at 4°C, the supernatant was then discarded, 500µl ethanol were added to the pellet and the mixture was again centrifuged at 14000rpm for 10 minutes. The supernatant was discarded immediately and the pellet was air-dried. The dried pellet was dissolved in 40µl dH2O.

Buffers:

S1 Resuspenson buffer	Macherey-Nagel
S2 Lysis buffer	Macherey-Nagel
S3 Eluation buffer	Macherey-Nagel

3.2.1.7. NucleoBond Plasmid Purification (Midi Prep)

Protocol:

Bacteria was cultured overnight in 120ml LB medium and harvested by centrifugation at 6000rpm for 15 minutes at 4°C. The cell pellet was carefully resuspended in 4ml S1 buffer (RNAse added) and placed in a 50ml Falcon tube. Subsequently, 4ml S2 buffer were added to the mixture and incubated at room temperature for 3 minutes. Then, 4ml pre-cooled S3 buffer were added and the mixture was incubated on ice for 5 minutes. At the same time, an AX 500 (Maxi) column was equilibrated with 2.5ml N2 buffer. Afterwards a pre-wetted Nucleobond folded filter was placed in a funnel and placed on the column. The bacterial lysate was loaded onto the filter and the column was washed with 10ml N3 buffer. The bound plasmid DNA was eluted in 5ml N5 buffer and collected in a 10ml Falcon tube. To precipitate the eluted DNA 3.5ml isopropanol were added, mixed carefully and centrifuged for 30 minutes at 4600rpm at 4°C. The supernatant was discarded, while 2ml ethanol were added to the cell pellet. The mix was briefly vortexed and centrifuged at 4600rpm for 10 minutes at room temperature. All ethanol was carefuly removed by pipetting and the pellet was allowed to dry. Finally, the dry pellet was dissolved in 40µl dH2O.

Material:

Sorvall RC 5C Plus	Sorvall® centrifuges
Sorvall SLA3000	Sorvall® centrifuge rotors
250ml Sorvall tubes	Sorvall® tubes
AX 500 (Maxi) column	Nucleobond® columns
Nucleobond folded filter	NucleoBond® filters
Rotanta 460	Hettrich Zentrifugen AG

Buffers and Medias:

S1 Resuspenson buffer	Macherey-Nagel
S2 Lysis buffer	Macherey-Nagel
S3 Eluation buffer	Macherey-Nagel
N2 Wash buffer	Macherey-Nagel
N3 Elution buffer	Macherey-Nagel
N5 Elution buffer	Macherey-Nagel

3.2.1.8. Polymerase Chain Reactions (PCRs)

3.2.1.8.1. Expand High Fidelity PCR System

The Expand High Fidelity PCR Kit (Roche®) includes the following contents:

- Expand High Fidelity Enzyme Mix∗
- Expand High Fidelity buffer (10x) with 15 mM MgCl2
- Expand High Fidelity buffer (10x) without MgCl2
- MgCl2 25 mM Stock Solution

∗ Enzyme storage buffer: 20mM Tris-HCl, pH7.5 (25°C), 100mM KCl, 1mM Dithiothritol (DTT), 0.1 mM EDTA, 0.5% Nonidet P40 (v/v), 0.5% Tween 20 (v/v), 50% glycerol

Additional Material:

- dNTP-Mix (deoxynucleotide mix)
- 0.2 ml thin-walled PCR tubes (Axygen PCR 02-C)
- Thermal block cycler (Applied Biosystems GeneAmp® PCR System 2700)

The PCR reaction mix was prepared according the Expand High Fidelity PCR System protocol:

Volume	Reagent	Final Concentration
4.125µl	dH2O	
2.5µl	10x Expand High Fidelity buffer (without MgCl2)	
5µl	MgCl2 (25mM)	
2µl	dNTP-Mix	200µM
1µl	dsDNA template	1-10ng
5µl	Forward primer	300nM
5µl	Reverse primer	300nM
0.375µl	Expand High Fidelity enzyme mix	1.7U/reaction

Thermal cycling:

	Cycles	Temperatur	Time
Initial Denaturation	1x	94°C	5 min
Denaturation		94°C	2 min
Annealing	30x	55°C	30 s
Elongation		72°C	2 min
Final Elongation	1x	72°C	7 min
Cooling		4°C	∞

3.2.1.8.2. Site-directed Mutagenesis

"In vitro" Stratagene QuickChange® Site-Directed Mutagenesis is a method to generate point mutations that can lead to amino acid changes and/or deletions or insertions of single or multiple amino acids. The standard method developed by Stratagene utilizes a supercoiled double-stranded DNA vector and two synthetic oligonucleotide primers featuring the desired mutation (see Figure 7). Mutation primers were designed according to recommendations of the Stratagene QuickChange® Site-Directed Mutagenesis manual and synthesized by Microsynth AG. Site-directed mutagenesis was also accomplished according to recommendations using the Stratagene QuickChange® Site-Directed Mutagenesis Kit with a PfuTurbo, Pfu Ultra or Pfu Ultra II DNA polymerase (2.5 U/µl).

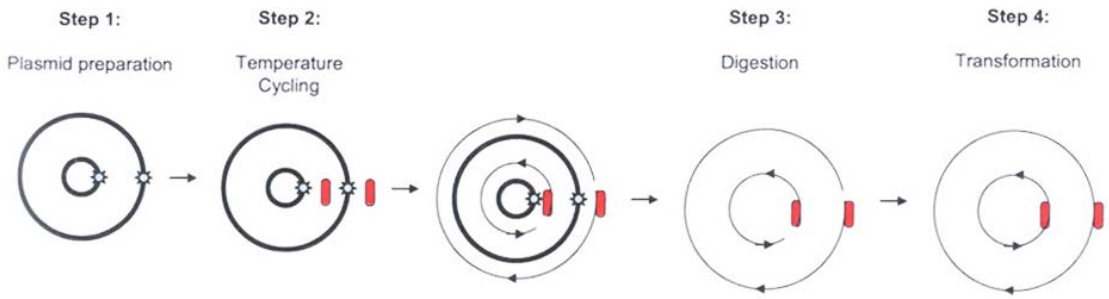

Figure 7; Overview of the site-directed mutagenesis method

(Adapted from Stratagene QuickChange® Site-Directed Mutagenesis Kit manual)

Step 1: The procedure utilizes a gene on a plasmid with the target site for mutation. Step 2: Two synthetic oligonucleotide primer containing the desired mutation anneal to the denaturated plasmid and are extended during temperature cycling by a PfuTurbo, Pfu Ultra or Pfu Ultra II DNA polymerase. Step 3: Incubation with Dpn1 is required to digest the parental methylated and hemimethylated DNA template. Step 4: Finally, nicked DNA containing the desired mutation is transformed into highly competent *E.coli* XL-blue cells.

The PCR reaction mix was prepared according the Stratagene QuickChange® Site-Directed Mutagenesis protocol:

5µl	10x Reaction buffer
1µl	dNTP-Mix
5-50ng	dsDNA template
125ng	Forward primer
125ng	Reverse primer
1µl	Pfu polymerase

dH2O was added to a final concentration of 50µl

Thermal cycling:

	Cycles	Temperatur	Time
Initial Denaturation	1x	95°C	30 s
Denaturation		95°C	30 s
Annealing	18x	55°C	1 min
Elongation		68°C	1.5min/kb of plasmid length
Cooling		4°C	∞

To digest the parental DNA the mix was incubated with 1µl DPN1 for 1 hour at 37°C.

The Stratagene QuickChange® Site-Directed Mutagenesis Kit includes the following contents:

- DNA polymerase (2.5U/µl)
- 10x Reaction buffer

Additional material:

- dNTP-Mix (deoxynucleotide mix)	
- 0.2 ml thin-walled PCR tubes	Axygen PCR 02-C
- Thermal block cycler	Applied Biosystems GeneAmp® PCR System 2700

3.2.1.9. Preparation of chemically competent *E.coli* cells

To acheive a better transformation efficiency, *E.coli* cells were converted into chemically competent cells according the following protocol:

3ml LB medium was inoculated with XL1blue *E.coli* strain and incubated over night at 37°C. The overnight culture was added to 500ml SOB++ medium and incubated at 25°C until the absorbance at 600nm was 0.5. The culture was kept on ice for 10 minutes. The cell suspension was centrifuged at 4500rpm for 10 minutes at 4°C. The resulting pellet was resuspended in 100ml ice-cold TB buffer. The suspension was again kept on ice for 10 minutes. After centrifugation at 4500rpm for 10 minutes at 4°C, the pellet was gently resuspended in 18.6ml ice-cold TB buffer complemented with 1.4ml DMSO. The mix was incubated on ice for 10 minutes. The suspension was aliquoted in pre-cooled Eppendorf tubes (600µl per tube), shock-frozen in liquid nitrogen and stored at -80°C.

Material:

Cuvettes (halb-mikro)	Greiner Bio One
Genesis 10UV scanning	Digitana AG thermo spectronic systems
Sorvall RC 3C Plus	Sorvall centrifuges
Sorvall HRL6	Sorvall rotors
Nalgene 1000ml tubes	

Buffers and Medias:
LB medium
SOB++ medium
TB buffer

Chemical Reagents:
DMSO

3.2.1.10. Heat-shock transformation of chemically competent *E.coli* cells with plasmid DNA

Transformation is a method to get foreign DNA into a recipient bacteria cell.

Protocol:
50µl of chemically competent cells were thawed on ice and mixed with 1 to 10µl of a solution containing the plasmid DNA. The mix was kept on ice for 30 minutes before heat shocked at 42°C for 45 seconds on the heating block. After the cells were again incubated on ice for 90 seconds, 400µl of SOC medium were added. The cells were then cultured in the shaking incubator at 37°C for 40 minutes. The cell suspension was then spread on agar plates by small sterile glass beads.

Buffers and Medias:
SOC

Bacteria cells:

E.coli XL1blue	were present in the Stucki lab
E.coli BL21 pLys S	were present in the Stucki lab

3.2.1.11. Sequencing

Mini Plasmid Preparations (Mini Preps) were sequenced by Microsynth GMBH, using standard sequencing primers provided by Microsynth. The plasmid DNA was diluted in dH2O to an end concentration of 0.8µg/10µl.

3.2.2. Protein manipulations

3.2.2.1. Determination of protein concentrations by Bradford or Lowry

To determine protein concentrations of cell extracts, two different methods were used dependening upon how the cell extracts were prepared. While protein concentrations of SDS extracts were measured by the Lowry assay, the Bradford analysis method was used for NP40 extracts, respectively. In both assays the absorbance (Bradford: 595nm, Lowry: 750nm) of four Bovine Serum Albumin (BSA) standard solutions was first measured to calculate a standard curve of absorbance. This resulting curve was used to determine the protein concentration of the samples.

Material:

Cuvettes (halb-mikro)	Greiner Bio One
Genesis 10UV scanning	Digitana AG thermo spectronic systems
Albumin from bovine Serum, Biochemika Fraction V	Fluka Chemie AG

3.2.2.2. NP40 Extract

The NP40 extraction method is not as harsh as the SDS extraction because proteins are not denatured in the process and interactions between proteins can still be analyzed. In contrast, the total amount of proteins obtained is smaller, because only soluble proteins can be extracted by this method.

Protocol:
Cells were washed in PBS and trypsinized. After inhibiting trypsin with DMEM, the cell suspension was centrifuged for 1 minute at 1500rpm. Subsequently, the pellet was washed twice with PBS before

the cells were resuspended in 100µl Buffer E (10cm plate). The suspension was frozen at -80°C and thawed on ice again. After the cells were spun down at 14000rpm for 10 minutes the supernatant was used for further experiments.

Buffers and Medias:
Buffer E
DMEM (incl. 10% FCS, 1% Pen Strep)
PBS
Trypsin-EDTA

3.2.2.3. SDS Extract

Protocol:
Cells were first washed with PBS before 250µl of Extraction buffer were added, so that the cells could be scratched off with the rubber spatula. In order to lower viscosity of the cell extract, it was passed several times with force through a small syringe needle which resulted in sharing of the chromatin. This was repeated until the viscosity was low enough to allow pipeting. An aliquot of 10µl was removed and protein concentration was analyzed by Lowry assay.

Buffers and Medias:
Blue dye
Extraction buffer
PBS
Solution A
Solution B

3.2.2.4. Western Blot

Western Blot is a technique, where proteins separated by SDS-PAGE are transferred onto a membrane and subsequently detected by immunological methods.

Protocol:
The SDS-gel was transferred on a nitrocellulose membrane for 1 hour with 250mA using the Mini Trans-Blot Cell from Bio Rad. To evaluate marker bands and success of blotting procedure the membrane was stained with Ponceau S. The blot was then incubated with 5% TBST-milk for 2 hours to block unspecific binding sites for the antibodies. Subsequently, the membrane was washed three times with TBST, before the primary antibody, diluted in 2.5% TBST-milk was added. The incubation was done on a parafilm coated glass plate in a wet chamber for time periods between 4 hours and overnight. The membrane was washed three times in TBST and was incubated for one hour with the secondary antibody which was also diluted in 2.5% TBST-milk (1:5000). After the incubation, the blot

was washed three times in TBST again. 1ml of ECL Western Blot detection solution (1:1 mix) was added to the blot for 1 minute. Then, the membrane was immediately wrapped into saran foil and exposed to X-ray films.

When the membrane was incubated with another primary antibody the blot had to be stripped first for one hour in stripping buffer. Before incubation with the primary antibody the blot was washed three times in TBST.

Material:	
Mini Trans-Blot cell	Bio-Rad blotting systems
Power Pac 200	Bio-Rad power supplies
Nitrocellulose membrane	GE Water & Process Technologies
Typon optimax	Raymed Imaging AG
Contatyp medical X-ray film	Typon Holding AG

Buffers and Medias:	
ECL (two solutions, mixed 1:1)	Amersham Biosciences
TBST	
5% TBST-milk	
Transfer buffer	
Stripping buffer	

3.2.2.5. Silver Staining of protein gels

Protocol:
First the gel was incubated in 100ml of 50% methanol for 15 minutes, then in 100ml of 5% methanol for 15 minutes and in 100ml dH2O containing 3.2µl of 1M DTT for 15 minutes. The gel was briefly washed in dH2O twice. Afterwards a little silver solution was added and poured away before the gel was incubated with the rest of the silver solution for 15 minutes. Again the gel was shortly washed twice with dH2O, followed by two short washing steps with developing solution. The gel was then incubated with the rest of the developing solution until the bands reached the desired intensity. To stop the chemical reaction solid citric acid was slowly sprinkled into the solution until the fizzing ceased. Finally, the gel was washed three times in dH2O for 15 minutes.
All incubations were carried out in fresh made solutions in a clean plastic box at room temperature with gentle shaking on a shaking platform.

Buffers and Medias:
50% methanol
5% methanol
Silver solution
Developing solution

Chemical reagents:
DTT
Nitric acid

3.2.2.6. Pull down arrangement

All pull downs were arranged according the following protocol:
The frozen cell pellet was thawed on ice before resuspended in 1.5ml NTEN buffer. The suspension was incubated on ice for 10 minutes again. The cell extract was cleared by centrifugation with 14000rpm, at 4°C for 10 minutes. The supernatant was decanted into a 2ml Eppendorf tube, while the pellet was discarded. The supernatant was incubated with different amount of equilibrated beads (between 20 and 40µl of αFlag M2 agarose, S-protein agarose, Streptavidin agarose*) for at least one hour at 4°C with agitation. Equilibration means to wash beads three times for fife minutes with NTEN buffer. After the incubation the tube was centrifuged at 1500rpm so that beads assembled at the bottom. The supernatant was discarded and beads were washed three times in 1.5ml NTEN buffer. For each washing step, beads were placed on the shaker for 5 minutes. 25µl SDS loading buffer were added to the washed beads and heated up to 100°C for 3 minutes on the heating block. Samples were loaded on an SDS gel in order to analyze them by Western Blotting or by silver staining.

*To assemble beads in pull downs using Streptavidin dynabeads, the tube was placed on the magnetic hanger instead of centrifugation.

Buffers:
NTEN buffer
SDS loading buffer

Chemicals:
αFlag M2 agarose
S-protein agarose
Streptavidin agarose
Streptavidin dynabeads

3.2.2.7. Production of GST-fusion proteins

Protocol:

Transformed BL21 pLys S bacteria cells were cultured in 500ml LB-medium containing ampicillin (50µg/ml) until they reached an OD600 of 0.6. 50µl IPTG of a 0.5M stock solution were added which initiated the expression. Three hours after the expression start the cells were collected by centrifugation and the pellet was frozen (-80°C) twice and rethawed. The pellet was then resuspended in 10ml E1A lysis buffer and was sonicated until the color of the extract changed to opaque. After centrifugation, the supernatant was incubated with 1ml of 50% equilibrated GSH-Sepharose for 15 minutes at 4°C. The mixture was poured into a glass wool filter column (self-made) followed by six washing steps with 5ml ELB buffer. The fusion protein was eluted by the addition of six times 0.5ml of a 20mM GSH solution, resulting in six different fractions. The protein quality was estimated by a coomassie stained SDS-PAGE. The fractions with the highest protein concentration were pooled and dialysed against Dialysis buffer using the Spectra/Por Dialysis Membrane for 4 hours. Finally, the concentration was measured by Bradford analysis and diluted to 1mg/ml.

Material:

Cuvettes (halb-mikro)	Greiner Bio One
Genesis 10UV scanning	Digitana AG thermo spectronic system
Cell disrupter B15	Branson sonifier
250ml Sorvall tubes	Sorvall tubes
Sorvall RC 5C Plus	Sorvall centrifuges
Sorvall SLA 1500	Sorvall rotors
Spectra/Por Dialysis Membrane 3500 MWCO	Spectrumlab

Buffers:

Dialysis buffer
E1A lysis buffer
ELB buffer
1x TBS buffer

Chemical Reagents

Ampicillin
10% glycerol
GSH (20mM)
GSH-Sepharose
IPTG
LB-medium

3.2.2.8. ATM Kinase Assay

Protocol:

To immuno precipitate ATM, 100µl HeLa nuclear extract (HNE), 100µl Buffer D and 200µl IP buffer were mixed, complemented with 1µl TOM α-ATM antibody and incubated for 2 hours at 4°C. 25µl Protein A-Sepharose (50% equilibrated with IP buffer) were added and incubated for 2 hours at 4°C. The solution was washed four times with 1ml IP buffer followed by two washes with 1ml kinase buffer. After the last wash the supernatant was completely decanted and the beads were resuspended in 17µl kinase buffer and 1µl of the GST-fusion protein (wild type and T4A mutant MDC1 FHA domain) was added. The reaction was initiated by the addition of 2µl of ATP (0.5mM) spiked with 0.5µl γ32P-ATP (3000 Ci/mmol) and maintained for 30 minutes at 30°C. Subsequently, the mix was centrifuged at 14000rpm for 1 minute. To stop the reaction 10µl of SDS loading buffer were added to 20µl of the supernatant and heated at 100°C for 3 minutes. All samples were loaded on a 12% acrylamid gel. The gel was fixed (40%MetOH, 10% acetic acid) and soaked in Enlightening Solution. The gel was then exposed to X-ray film overnight.

Buffers and Medias:
Buffer D
IP buffer
Kinase buffer
SDS loading buffer

Chemical Reagents:
Acetic acid
TOM α-ATM antibody
ATP
Enlightening solution
γ32P-ATP
HeLa nuclear extract
MetOH
Protein A-Sepharose

3.2.3. Manipulations with human cell lines

3.2.3.1. Calcium phosphate transfection

In general, transfection is a method to bring foreign DNA into cells of higher eukaryotes.

To transiently express desired proteins in human cells, 293T transformed human embryonic kidney cells were transfected by calcium phosphate. Because the transfection efficiency is best when the cell are about 50% confluent, cells were split on the previous day so that they reached 50% confluency on the day of transfection. A glass coverslip was placed in each dish to control the efficiency of the transfection by fluorescent microscopy.

Preparations:
The required amount of DNA (1µl/µg) was first diluted in dH2O. This mix was slowly added to 2x HBS prepared in a 10 ml Falcon tube. Subsequently, the CaCl2 solution was carefully added to the mix under gentle agitation of the falcon tube.

Mixing proportions depend on dish size:

Plate size	2x HBS	DNA (1µl/µg)	dH2O	CaCl2(2M)
6-well plate	100µl	2-5µg	87.5µl	12.5µl
Small dish	240µl	5-10µg	210µl	30µl
10cm dish	660µl	10-35µg	577.5µl	82.5µl
15cm dish	1400µl	20-30µg	1225µl	175µl

The mix was dropwise added to the cells and the culture was incubated at 37°C. After 24 hours of incubation the cells were washed once with PBS and then fresh medium was added. The cells were collected 48 hours past transfection and used for experiments.

Buffers and Medias:
2x HBS (pH adjusted to 7.09 with NaOH)
2 molar CaCl2 solution

3.2.3.2. Lipofectamin transfection

Lipofectamin transfection was carried out to get stably transfected cell lines. Best transfection efficiencies were achieved around 50% confluency in 6cm dishes. U2OS cells were used to retrieve stably transfected cell lines.

Preparations:
300µl Optimem and 15µl Lipofectamin were mixed and incubated for 10 minutes at room temperature. At the same time 300µl Optimem were mixed with 4µl DNA (1µl/µg). The two Optimem solutions were brought together and incubated for 20 minutes at room temperature. Subsequently, the cells were washed once with PBS and 3ml of pre-warmed DMEM containing 5% FCS were added. The DNA-Lipofectamin was added dropwise to the 6cm dish.
The next day the medium with 5% FCS was replaced with normal DMEM containing 10% FCS and antibiotics.

Buffers and Medias:
DMEM
FCS
Lipofectamin
Optimem
PBS

3.2.3.3. DAPI staining

DAPI (4,6-Diamidino-2-phenylindol) is a fluorescent dye that stains DNA. Hence, it is used as a marker of the nucleus in fluorescence microscopy.

Protocol:
Cells grown on coverslips, were washed twice with PBS before they were fixed in 50% methanol for 10 minutes at 4°C. Subsequently, cells were washed twice with PBS, before the coverslips were placed cells-down on a drop of DAPI solution on parafilm. Coverslips were incubated in the dark for 10 minutes and washed twice with PBS. Then, the coverslips were mounted on a microscopy slide with a drop of vectashield. The coverslips were immobilized on the slide by transparent nail polish.

Material:
Coverslips
Glass slides
Fluorescence microscope

Buffers and Medias:
PBS
50% methanol
Nail polish
DAPI
Vectashield

3.2.3.4. Selection of stably expressing cell clones

In order to isolate stably transfected cell clones, the transfected cells were selected by means of an antibiotic resistance gene located on the expression construct.

Protocol:
After Lipofectamin transfection cells grew for two days on a 6 cm plate. The dish was washed once with PBS before 500ml trypsin-EDTA was added. After a short incubation period 3.5ml of medium were pipetted into the dish and the rest of the unsolved cells were released from the surface. Four 10cm dishes were prepared by adding 10ml medium containing G418 (90µl/ml). The cell suspension was diluted in three different ratios (1:10, 1:20, 1:33). The three dilutions were partitioned between three 10cm dishes. Non-transfected cells diluted at 1:10 ratio were resuspended in the fourth dish as a negative control.
When the cell colonies reached a certain dimension, the cells were picked under the microscope. The individual clones were transferred to a 24-well plate that contained a coverslip in each well. After the clones reached a high density, coverslips were removed and the transfection success was controlled by fluorescence microscopy.
Clones with the highest expression levels were expanded and frozen at -80°C. Extracts were prepared as described above.

Buffers and Medias:
DMEM (incl.10% FCS, Pen-Strep)
G418
PBS
Trypsin-EDTA

Material:
24-well plate
6/10/15cm dishes
Coverslips

4. Goals of the thesis

4.1. Identification of an ATM phosphorylation site in MDC1

Previous data in our lab showed that MDC1 is phosphorylated in the N-terminal region by ATM. Two potential phosphorylation sites exist at the N-terminus of human MDC1: Thr4 and Thr98. Since deletion of the first nine amino acids of an N-terminal MDC1 fragment (1-124) resulted in a protein that could not be phosphorylated by ATM in vitro, we assumed that Thr4 is the only residue that is targeted by ATM. Thus, the goal of this project was to directly prove that threonine 4 is the actual residue at the MDC1 N-terminus that is phosphorylated by the ATM kinase.

4.2. Development of a tandem affinity purification system in order to identify novel FHA and BRCT interaction partners

The aim of the second project was to develop an "*in vivo*" pull down strategy to identify novel components of the DNA damage response. Many proteins involved in the DNA damage response feature conserved domains, such as FHA or BRCT domains that interact with other proteins in a phosphorylation-dependent manner. To detect novel interaction partners of such domains, we aimed to develop a strategy to trap them by overexpressing these domains in mammalian cells as tagged fusion proteins, followed by tandem purification and identification of interaction partners by mass spectrometry. As a first step, the goal of this thesis was to design the system and to test it in a proof-of-principle set up.

Since three phospho-specific interaction partners for BRCA1 BRCT domains have already been identified (CtIP, Bach1 and RAP80; see also introduction), we decided to over express affinity-tagged BRCA1 BRCT domains as a bait in human cells to test if we could retrieve any of these proteins by our "*in vivo*" pull down strategy.

5. Results

5.1. Identification of an ATM phosphorylation site in MDC1

5.1.1. Introduction

Previous data from our lab showed that deletion of the first nine amino acid residues of MDC1 prevented phosphorylation of a recombinant N-terminal fragment of MDC1 by ATM. In order to directly show that T4 is targeted by ATM *in vitro*, Thr4 was replaced by Ala by site-directed mutagenesis and the protein was produced in bacteria. Finally, the purified protein was subjected to an *in vitro* ATM kinase assay to test whether replacement of Thr4 would affect the phosphorylation.

Originally, we planned to mutate the Thr4 residue to Ala in an N-terminal MDC1 GST fusion construct (amino acids 1-124; Spycher et al., 2008) using the Stratagene QuickChange® Site-Directed Mutagenesis Kit. However, even after several attempts, the mutagenesis was not successful. Thus, an alternative approach was established.

To generate a GST fusion protein, a fragment of the MDC1 cDNA comprising the N-terminal FHA domain (aa 1-154) and bearing a T4A point mutation (generated by Stephanie Jungmichel) was subcloned into the pGEX4T3 bacterial expression vector. The pGEX4T3 vector already contains a GST tag in frame with a multiple cloning site.

Since the restriction sites in the original plasmid (PEYFPnucTO_MDC1-FHAT4A) were not compatible with the pGEX vector, the fragment featuring the first 124 amino acids was isolated by the Expand High Fidelity PCR System. The utilized primers; M-1 T4A_fw and M_FHA_rev were provided by Stefanie Jungmichel and Christoph Spycher. The pGEX4T3 bacterial expression vector (GE Healthcare Bioscience) was linearized by digestion with BamH1 and Xho1. The vector was then purified by NucleoSpin® Gel-Extraction. To clone the T4A mutated MDC1 FHA domain into the empty vector, the purified PCR fragment bearing the mutation was also digested with BamHI and XhoI, followed by ligation with T4 DNA ligase. The ligation reaction was transformed into *E.coli* XL1blue cells. Plasmid DNA isolated by a mini prep was test-digested with BamH1 and Xho1 in order to verify the ligation success.

All 7 tested *E.coli* clones contained the vector and the insert (see Figure 8). Best results (clone Nr. 4 and 7) were sent for sequencing to the Microsynth GmbH. Sequencing results revealed that the sub-cloning was successful (see appendix sequence report of the T4A mutant N-terminal fragment of MDC1).

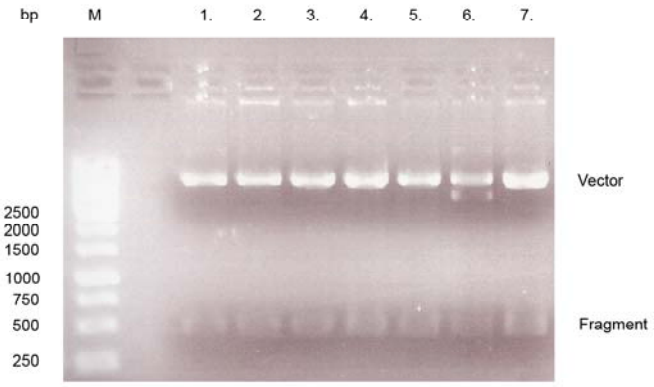

Figure 8; The test digest with BamH1 and Xba1 revealed a successful subcloning.
5µl of the 1kb marker and 10µl of the test digestion mix were loaded on a 1% agarose gel. The calculated size of the fragment is 469pb. M 1kb marker, 1.-7. samples.

E.coli BL21 pLys S cells were transformed with pGEX4T3 carrying the T4A mutant fragment (pGEX4T3-MDC1-FHA(T4A)). In parallel, the wild type fragment (pGEX4T3-MDC1-FHA(WT)) was also purified as a positive control. Cells were cultured in LB to an OD600 of 0.6 before the expression of the GST-fusion protein was induced by IPTG. GSH-sepharose was used for the purification of the fusion protein. Subsequently, protein quality and quantity was estimated by SDS-PAGE and coomassie blue staining. Elution fractions 2 to 6 were pooled and diluted to 1µg/µl after the concentration was determined by the Bradford assay. In conclusion, the mutant as well as the wild type fusion protein was strongly expressed and well purified (see Figures 9 and 10), so they could be directly used for the intended experiments.

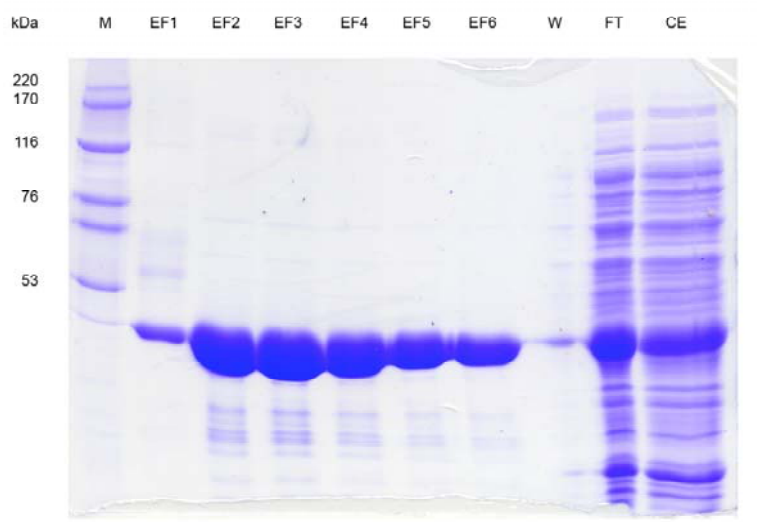

Figure 9; The T4A mutant fragment was well expressed

The pGEX 4T3 vector bearing the T4A mutant fragment was transformed into *E.coli* BL21 pLys cells and the expression was induced by IPTG. The protein was purified using GSH-sepharose. 5µl of the high molecular weight (HMW) marker, 5µl of each elution fraction (EF) 1-6, 5µl wash (W), 5µl flow through (FT) and 5µl cell extract (CE) were loaded on a 10% SDS gel. The calculated size of the fusion protein is around 40kDa.

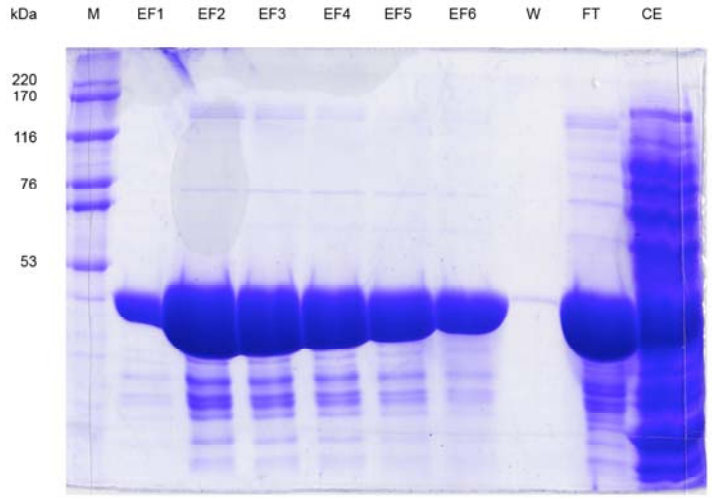

Figure 10; The wild type fragment was very well expressed

The wild type protein was also transformed into *E.coli* BL21 pLys cells and the expression was induced by IPTG. The wild type protein was purified using GSH-sepharose. 5µl of the high molecular weight (HMW) marker, 5µl of each elution fraction (EF) 1-6, 5µl wash (W), 5µl flow through (FT) and 5µl cell extract (CE) were loaded on a 10% SDS gel. The calculated size of the fusion protein is around 40kDa.

5.2.2. T4 is the only *"in vitro"* ATM phoshorylation site at the N-terminus of MDC1

For the *in vitro* kinase assay, ATM was immunoprecipitated from HeLa nuclear extract by a rabbit anti human ATM polyclonal antibody, bound to Protein A-sepharose. Immunoprecipitated ATM was incubated with either the mutant or the wild type GST-fusion protein. Fusion proteins were also incubated with simply kinase buffer as a control. The phosphorylation reaction was initiated when radioactive ATP was added. The reaction mix was loaded on an SDS gel. Finally, the gel was dried and exposed to film overnight. As expected, the wild type fragment was efficiently phosphorylated by ATM in vitro whereas the T4A mutant MDC1 FHA domain could not be phosphorylated by ATM (Figure 11; compare lane 2 and lane 4). Thus, the results of this *in vitro* ATM kinase assay provide conclusive evidence that *in vitro*, Thr4 is the only ATM phosphorylation site at the N-terminus of MDC1.

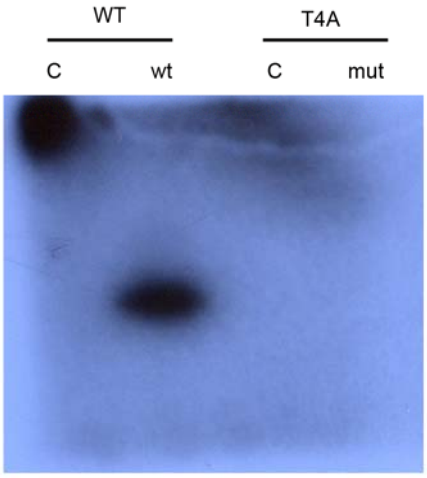

Figure 11; The T4A fragment is not phosphorylated by ATM

ATM was immunoprecipitated from HeLa nuclear extract. ATM resuspended in 17µl kinase buffer was incubated with 1µl of either the mutant or the wild type GST-fusion protein (1µg/µl). 1µl of fusion proteins were also incubated with simply kinase buffer as a control. The phosphorylation reaction was initiated when 2µl of ATP spiked with 0.5µl of γ32-ATP (3000Ci/mmol) were added. The reaction mix was incubated for 30 minutes at 30°C before the whole amount (20µl) was loaded on a 12% SDS acrylamide gel.

5.2 Development of a tandem affinity purification (TAP) system for FHA and BRCT domains

5.2.1 Introduction

FHA and BRCT domains are known phosphorylation-dependent protein interaction modules (see introduction). However, only few *bona-fide* interaction partners for FHA and BRCT domain proteins have been identified to date. Therefore, we decided to search for novel interaction partners that bind to these domains in a phosphorylation-dependent manner in order to identify novel components of the DDR. To perform this biochemical screen, proteins must be exceedingly purified, so we set up a tandem affinity purification (TAP) system as this method was described in a recent published study revealing new interaction proteins of the RAD53 FHA domain (Smolka et al., 2006). A TAP is a two-step pull down method based on different short peptide tags and their corresponding affinity matrix. In contrast to the most frequently employed TAP system using the TEV protease for the first elution procedure, we have chosen a Strep-tag II that can be physiologically eluted with Biotin. The Strep-tag II is an eight-amino acid residue minimal peptide sequence consisting of Trp-Ser-His-Pro-Gln-Phe-Glu-Lys and shows intrinsic affinity toward Streptavidin (Schmidt and Skerra et al., 2007). The mild elution with biotin is replacing Strep-tag II from Streptavidine because of the higher Streptavidin binding affinity of Biotin. Such mild elution conditions in the first TAP purification step are required to assure the persistence of protein interactions. The second TAP purification step is using S- or Flag-tags and is designed to reach a higher purity level of the sample by reducing unspecific protein interactions (see Figure 12).

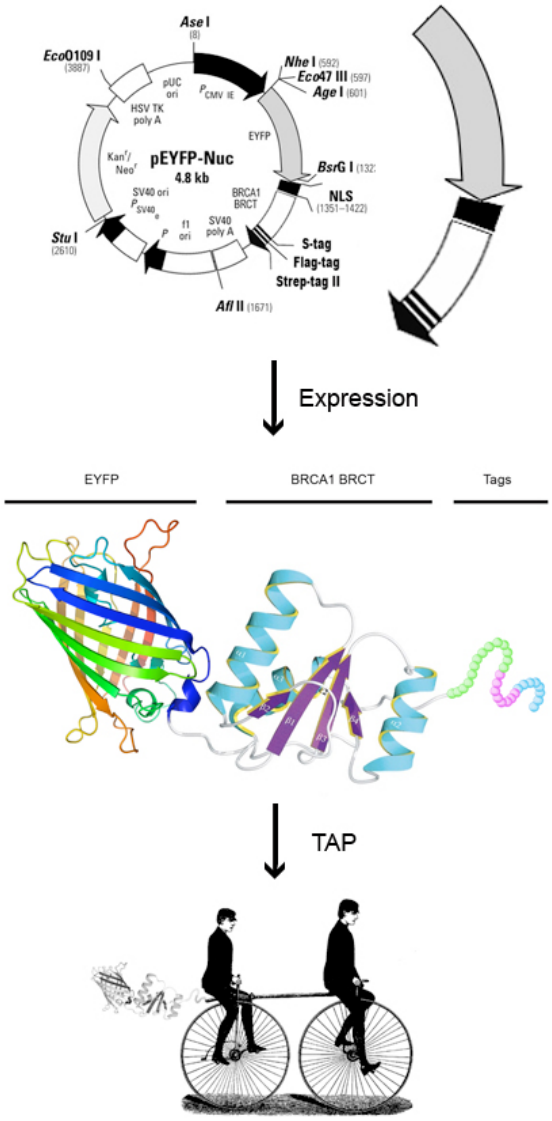

Figure 12; is a schematic illustration showing the human expression vector pEYFPnucTO with the subcloned BRCA1 BRCT domain including the tag triplet.

The vector will be transfected into human U2OS cells and expressed as a fusion protein featuring EYFP, the BRCA1 BRCT domain and the tag triplet. In order to find novel interaction partners involved in the DDR, the fusion protein will be purified by TAP.

The pEYFPnucTo mammalian expression vector was digested with XbaI and BamHI to create an empty vector. Oligonucleotides synthesized by Microsynth GMBH were used to insert tags into the empty vector. Oligonucleotides were designed in a way that the posterior XbaI restriction enzyme site was destroyed after the cloning step. Therefore, a new XbaI site was directly positioned behind the anterior BamHI site so that further inserts can be cloned into the vector using these two restriction enzymes. The oligonucleotides finally featured an S-tag, a central Flag-tag and a Strep-tag II

forming the tail of the fusion protein. As oligonucleotides are delivered as DNA single strands, they first needed to be annealed by passing through a descending temperature row (95°C for 30sec, 72°C for 2 min, 37°C for 2 min and 25°C for 2min). Oligonucleotides annealed under formation of an anterior "sticky end" that is compatible with a BamHI restriction site and a posterior "sticky end" that fits into the XbaI site. Oligonucleotides were phosphorylated by polynucleotide kinase (PNK). Annealed oligonucleotides were finally ligated overnight with the empty pEYFPnucTO vector (pretreated with CIP) and transformed into *E.coli* XL1blue. This modified vector was used to generate all further constructs.

In order to proof functionality of our "*in vivo*" pull down strategy, we decided to use a fragment comprising the BRCA1 BRCT domains (aa 1644-1864) as a proof-of-principle because three interaction partners for the BRCA1-BRCT domains have already been identified (CtIP, BACH1, Rap80; see introduction). The BRCA1 BRCT domain cDNA fragment was already available in a pEYFPnuc vector. Unfortunately, this construct contained a terminal stop codon, so the tags would not be expressed. Consequently, the BRCT domains were isolated by Expand High Fidelity PCR. PCR success was verified by agarose gel electrophoresis. A clear band was detectable at the size around 650bp, indicating that the PCR reaction was successful as the calculated size of the BRCA1 BRCT domain amounts to 667bp (see Figure 13). Best samples were purified by NucleoSpin® PCR clean up.

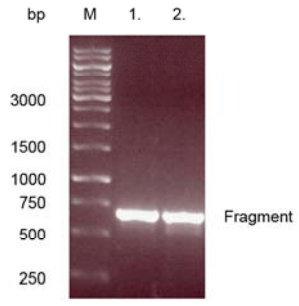

Figure 13; The BRCA1 BRCT domain was isolated by Expand High Fidelity

5µl of the PCR reaction as well as 3µl of the 1kb marker were loaded on an agarose gel to verify PCR success. The BRCT domain was isolated by Expand High Fidelity PCR using the following two primers: BRCA1_BRCT_for (available in the lab) and BRCA1_rev_noStop (ordered from Microsynth). M: 1kb marker

The fragment as well as the vector were subsequently digested with BamHI and XbaI. The vector was additionally treated with CIP for one hour to prevent self-ligation. Again samples were loaded on an agarose gel and the relevant bands were purified by NucleoSpin® gel extraction. Finally, the BRCA1 domain and the linearized pEYFPnucTo vector featuring the tags were ligated overnight and transformed into *E.coli* XL1blue cells. The plasmid was then isolated by a mini prep and subjected to a control digestion with BamH1 and Xba1 restriction enzymes. Unfortunately, the quality of the agarose gel was very bad. However, we could clearly detect the linearized vector at the size around 5.5kb. In order to detect a signal derived from the BRCA1 BRCT fragment, the exposure time had to be extremely increased. Consequently, the marker disappeared. However, marker bands visible at shorter exposure times revealed the BRCA1 BRCT fragment at its correct size around 650bp (see Figure 14). We sent clones Nr. 2 and 3 to Microsynth GMBH for sequencing (see appendix sequence report of the BRCA1 BRCT domain)

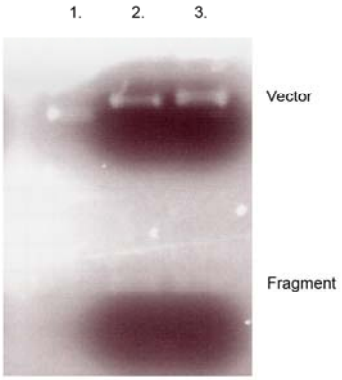

Figure 14; The BRCA1 BRCT domain was successfully subcloned into the pEYFPnucTO vector
The isolated fragment was subcloned into the empty pEYFPnucTO (featuring tags) and test digested with BamHI and XbaI. The marker is not visible due to the high exposure time. Clone Nr. 2 and 3 were sent to Microsynth GMBH for sequencing, 1.-3. samples.

Proteins may interact with unspecific components of a purification system. Thus, a procedure where the TAP assay is carried out in parallel with the wild type protein and a certain point mutant that abrogates phosphorylation-specific binding should help to distinguish between real interaction partners and unspecific binding proteins (comparative pattern analysis).

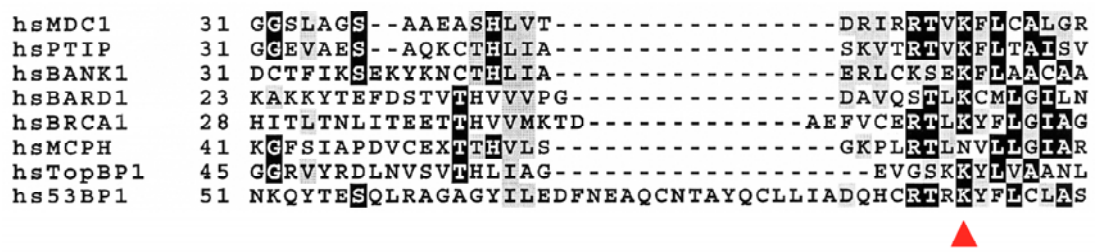

Figure 15; Lysine at position 1702 in BRCA1 is a conserved residue within BRCT domains
Sequence comparison of several BRCT domains from MDC1, PTIP, BANK1, BARD1, BRCA1, MCPH, TopBP1 and 53bp1 revealed a lysine at position 1702 in BRCA1 to be located in a highly conserved pattern with a crucial role for the maintenance of protein-protein interactions. The phosphorylation-dependent interaction is abrogated when Lys is replaced by a Met residue (Clapperton et al., 2004)

It was shown that BRCA1 BRCT-BACH1 interaction is abrogated by the K1702M mutantion (Clapperton et al., 2004) (see Figure 15). The K1702M mutation in the BRCA1 BRCT domain was introduced by the Stratagene QuickChange® Site-Directed Mutagenesis kit. Mutation primers (for_K1702M_BRCA1 and rev_K1702M_BRCA1) were designed according recommendations in the Stratagene QuickChange® Site-Directed Mutagenesis manual and synthesized by Microsynth GMBH. To digest the parental plasmid (pEYFPnucTo featuring tags and BRCA1BRCT) after the mutagenesis PCR, the mix was incubated with DPN1 that is specific for methylated bacterial DNA. In order to amplify the mutant plasmid, the PCR mix were transformed into *E.coli* XL1blue cells and DNA was isolated. An agarose gel was loaded and best results were sent to Microsynth GMBH for sequencing (see appendix sequence report of the K1702M mutant BRCA1 BRCT domain).

Midi preps were prepared from both vectors, as transfection of cells requires a large amount of plasmid DNA. First we transiently transfected human 293T cells by calcium phosphate transfection. Unfortunately, transfection efficiency was very poor even though the expression level of the few transfected cells was high. The attempt to purify the fusion protein by a Flag-tag pull down was not successful (data not shown). However, since this method didn't yield high transfection efficiency, we decided to generate a stable cell line expressing the tagged BRCA1-BRCT domains. Human osteosarcoma cell line U2OS cells were transfected according to the lipofectamin transfection protocol and subsequently selected by G418 antibiotic resistance.

Resistant clones were picked and transfection success was confirmed under the fluorescent microscope when the enhanced yellow fluorescent protein (EYFP) as a part of the fusion protein was expressed. The transfection efficiency was shown to be rather low and also the expression level is more or less weak. In some of transfected cells, nuclear dots were observable. These dots most likely represent the nucleoli (see Figure 16). Positive clones were transferred and cultivated in 15cm plates. The yield of one plate served as cell extract for one pull down experiment. Harvested cells were frozen in the -80°C until they were used for the pull down assays.

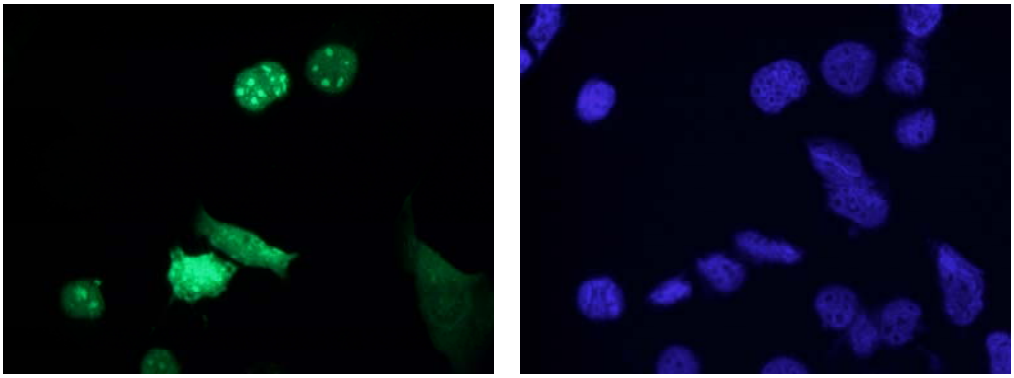

Figure 16; Transfection rate and expression levels were rather low

Human osteosarcoma U2OS cells were transfected with the pEYFPnucTO featuring the triple tagged BRCA1 BRCT domain. On the left side, transfected cells appear green due to the expressed EYFP. On the right side, nuclei of all cells shine in blue, as DAPI binds to DNA.

5.2.2. Pull down preparations

Cells were thawed on ice and resuspended in NTEN buffer. To clear the cell extract from insolubilized cell debris, insoluble membrane fragments and cellular matrix components, it was centrifuged at 14000rpm for 10 minutes. The supernatant containing the soluble proteins was now ready to be incubated with equilibrated beads.

5.2.3. Flag-tag pull down

We first purified the fusion protein by a singlestep affinity pull downs in order to confirm that all tags work fine. First we tested if the Flag-tag binds to mouse αFlag M2 agarose.

The cell pellet was resuspended in NTEN buffer and the cleared cell extract was incubated with equilibrated αFlag M2 agarose. Beads with bound proteins were washed three times with NTEN buffer. Samples were kept after each step so that the fusion protein could be traced through out the purification procedure. All samples were loaded on a gel and analyzed by silver staining as well as by Western Blotting. We used a polyclonal rabbit αFlag antibody as primary antibody in the Western Blot.

The calculated weight of the fusion protein is 57kDa. The Western Blot revealed a clear band in the eluate at the range around 60kDa, most likely representing the BRCT fusion protein. This strongly indicates that αFlag beads are able to pull down and enrich the Flag-tagged fusion protein. The weak band in the supernatant (SN) gives further evidence that the fusion protein binds to the beads and is no longer present in the supernatant. αFlag beads are coated with monoclonal mouse antibodies. After the SDS treatment these antibodies separate from the beads and solubilize in the eluate. When we use an αmouse antibody as a secondary antibody in the Western Blot, two strong bands appear in the eluate representing the light and the heavy chain of the M2 anti flag antibody. So we had to use the polyclonal rabbit αFlag antibody as a primary detection reagent of our fusion protein. Polyclonal antibodies do not work as specifically as monoclonal antibodies, consequently four non-specific bands appear in the blot. However, these four bands with sizes at 200kDa, 97kDa, 70kDa and 30kDa are only detectable in the cell extract and in the supernatant but not in the eluate. There are no bands observable in none of the washing fractions indicating that any or only little amount of the fusion protein gets lost during the washing procedure. Although the antibody should have the highest affinity towards the Flag-tag, the fusion protein appears weaker compared to the bands at 200 and 30kDa, again indicating that the expression level of the fusion protein was very low in these cells (see Figure 17).

Furthermore, to test the purification specificity and in order to detect BRCA1 BRCT interaction partners (known or unknown), a silver stain of a Flag-tag pull down was performed using α-Flag M2 agarose beads. The pull down was done the same way as for the Western Blot. The number and intensities of protein bands in the eluate reveal that many unspecific proteins are pulled down by the M2 Flag beads, indicating that a tandem purification is required to distinguish real interaction partners from unspecific background binding. Even though a clear band representing the fusion protein appeared in the Western Blot, there is no prominent band visible in the silver stain at around 60 kDa. This is probably due to a low expression level of the protein (see Figure 18).

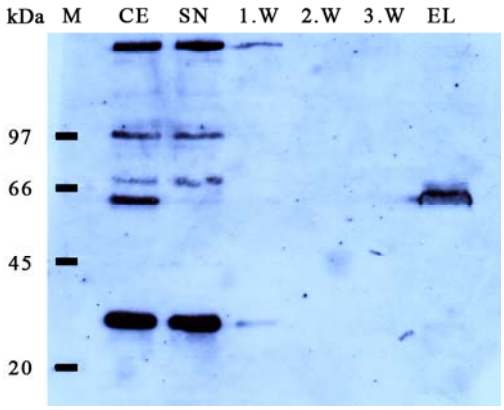

Figure 17; α-Flag M2 agarose beads are able to pull down flag-tagged fusion proteins.

20µl α-Flag M2 agarose beads were used in the pull down. Samples were loaded on a 10% SDS gel and the fusion protein was detected by Western Blot using a polyclonal rabbit α-Flag antibody diluted 1:300. The film was exposed for 30 minutes and the calculated size of the fusion protein is around 57kDa. M; low molecular weight marker, CE; Cell extract, SN; supernatant, W; washes 1-3, EL; eluate

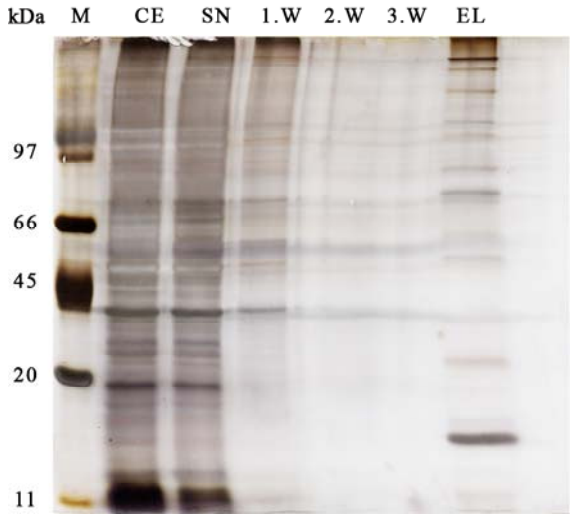

Figure 18; Silver staining revealed the Flag-tag pull down as rather unspecific

The Flag-tag pull down was performed using 30µl α-Flag M2 agarose. Samples were loaded on a 10% SDS gel and silver stained. M; low molecular weight marker, CE; Cell extract, SN; supernatant, W; washes 1-3, EL; eluate

5.2.4. GFP staining of a Flag-tag pull down

Due to the structural similarity of GFP and EYFP, some antibodies against GFP also cross react with EYFP. As expression control we performed a Western Blot using a polyclonal mouse α-GFP to immunostain EYFP as a part of the fusion protein. To this end, a Flag-tag pull down was performed and analyzed by Western Blot using the monoclonal α-GFP antibody. A strong signal in the elutae with a molecular weight corresponding to our fusion protein was detected, indicating that the fusion protein is efficiently enriched by the Flag pull down. However, the signal in the cell extract is weak indicating that the fusion protein is poorly expressed (see Figure 19).

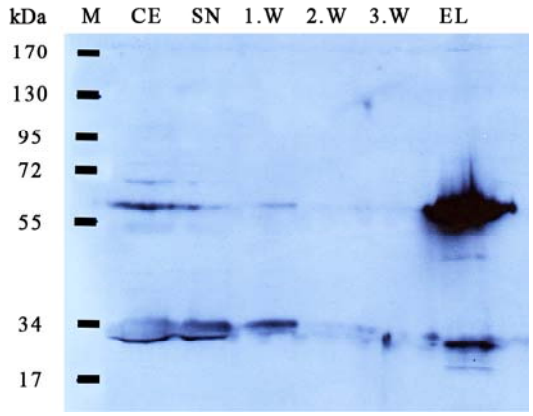

Figure 19; The fusion protein is weakly expressed but gets well enriched in the pull down
The pull down was performed using 40µl α-Flag M2 agarose beads. Samples were loaded on a 10% SDS gel. The monoclonal α-GFP antibody used in the Western Blot was diluted 1:1000 and the film was exposed for 30 minutes. M; low molecular weight marker, CE; Cell extract, SN; supernatant, W; washes 1-3, EL; eluate

5.2.5. S-tag pull downs

A single step pull down was also performed using protein S agarose in order to check functionality of the S-tag. The pull down was done as described for the Flag-tag pull down. The monoclonal α-Flag M2 antibody was used to detect the fusion protein by Western Blot. While the signal in the cell extract (CE) and also in the supernatant (SN) is only weak, the band representing the fusion protein in the eluate is very strong (see Figure 20). A closer look at the cell extract as well as at the supernatant disclose the fusion protein clearly appearing as a double band. The appearance of this double band was also observed in other pull downs (data not shown) suggesting that the BRCA1 BRCT domain exists in two isoforms with slightly distinct molecular weight. Alternatively, it is also possible that the fusion protein is partly modified, e.g. phosphorylated. This immunoblot also clearly demonstrated that the anti-Flag monoclonal antibody produced much less background than the polyclonal antibody, as only the band corresponding to the fusion protein can be detected. In conclusion, these data suggest that the S-tag works fine and the fusion protein can be efficiently enriched by S-protein agarose beads. Samples of a S-protein agarose pull down were also loaded on an SDS gel and silver stained analog to the Flag-tag pull down. The bands in the eluate are much weaker as compared to the Flag-tag pull down, however

one band at around 70kDa is clearly visible (see Figure 21). As the gel did not run entirely straight, this band might represent the fusion protein. However, this assay confirms a very low protein expression, as there is again no strong band observable in silver-stained SDS gels.

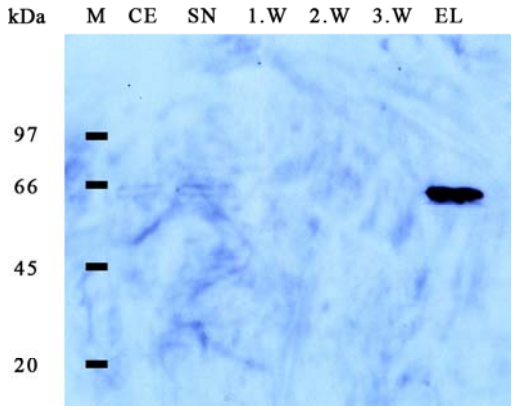

Figure 20; S-protein agarose is able to pull down the fusion protein

30µl S-protein agarose were used for the pull down. All samples were loaded on a 10% SDS gel. A monoclonal mouse α-Flag M2 antibody was used in the Western Blot. The film was exposed for 1 minute. M; low molecular weight marker, CE; Cell extract, SN; supernatant, W; washes 1-3, EL; eluate

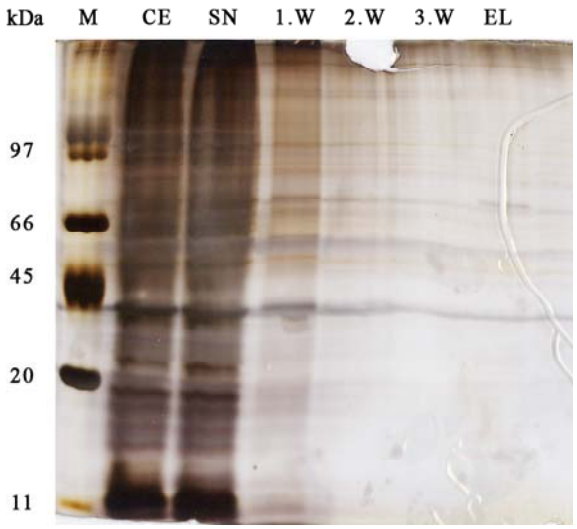

Figure 21; Silver stained SDS gel of an S-tag pull down revealed only weak bands in the eluate.

Samples of an S-tag pull down were loaded on a 10% SDS gel and silver-stained. The pull down was performed using 20µl protein S agarose beads. M; low molecular weight marker, CE; Cell extract, SN; supernatant, W; washes 1-3, EL; eluate

5.2.6. Streptavidin agarose and Streptavidin dynabead pull downs

To finally test the last but most important tag of the triplet, we performed a Strep-tag II pull down using streptavidin agarose. The pull down was again performed similar to the previous pull down assays. To detect the fusion protein, the monoclonal α-Flag M2 antibody was utilized for the Western Blot. There was unfortunately no band but a little smear observable in the eluate. Furthermore, it seems that Strep-tag II didn't bind to the streptavidin beads as the same amount of fusion protein is detected in the supernatant as in the cell extract (see Figure 22). The pull down was repeated several times in the same manner or with minor alterations but always ended up with the same result. A shorter exposure of the film revealed again the appearance of a double band in the cell extract and the supernatant. To confirm the inability of the Strep-tag II fusion protein to bind to streptavidin-coated beads, a further pull down was carried out using streptavidin dynabeads (see Figure 23). Now a clear band became visible in the eluate but not at the expected size, indicating that this is not our fusion protein. However, if the observed band is not the fusion protein, it must be another protein that unspecifically binds to the streptavidin-coated dynabeads and cross-reacts with the monoclonal α-Flag antibody. As there is no band detectable in the washing fractions and the band appearing in the supernatant shows the same intensity as the band the cell extract, we have to conclude that the Strep-tag II fusion protein for some reason doesn't bind efficiently to the streptavidin beads.

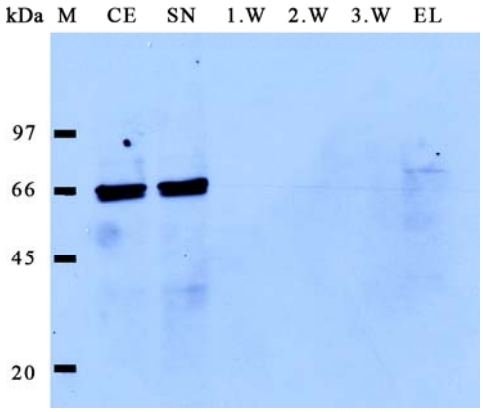

Figure 22; Streptavidin agarose beads are not able to pull down the Strep-tag II fusion protein
40µl Streptavidin agarose beads were used in the pull down. Samples were loaded on a 10% SDS gel and analyzed by Western Blot. We used the monoclonal mouse α-Flag M2 as primary antibody. The film was exposed over night. M; low molecular weight marker, CE; Cell extract, SN; supernatant, W; washes 1-3, EL; eluate

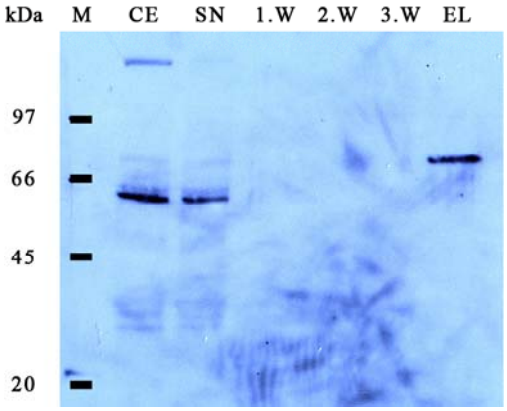

Figure 23; Streptavidin dynabeads are not able to pull down the Strep-tag II fusion protein
40µl Streptavidin dynabeads were used in the pull down. A 10% SDS gel was loaded and analyzed by Western Blot using the monoclonal mouse α-Flag M2 antibody. Exposure time was 30 minutes. M; low molecular weight marker, CE; Cell extract, SN; supernatant, W; washes 1-3, EL; eluate

6. Discussion

6.1. T4 is the only "*in vitro*" ATM phoshorylation site at the N-terminus of MDC1

Our lab has recently discovered that MDC1 is phosphorylated at its N-terminus. Deletion of the first nine amino acids of MDC1 abrogated this phosphorylation (Christoph Spycher, unpublished data). There is a conserved TQ motif within the first nine amino acids of MDC1 and TQ motifs are known consensus ATM target sites. Thus, we speculated that T4 might be phosphorylated by ATM. In addition there is another highly conserved TQ site located at the MDC1 N-terminus: Thr98. We also wanted to confirm that ATM only phosphorylates Thr4 and not both Thr4 and Thr98
In order to test this we created a GST fusion protein consisting of the first 124 amino acids of MDC1 and featuring the point-mutated T4A and subjected it to an "*in vitro*" ATM kinase assay. The results clearly revealed that the T4A mutant fragment was not phosphorylated by ATM. This indicates that ATM phosphorylates Thr4 in vitro. Furthermore, we can conclude that Thr4 is the only ATM phosphorylation site within the MDC1 N-terminus as the T4A fragment was not phosphorylated, even though Thr98 was still present.
The MDC1 FHA domain spans a region between amino acids 33-131 and is structurally organized into a six-stranded and five-stranded β-sheet forming a β-sandwich. However, Thr4 is not a component of this structural unit, so it may be readily accessible for phosphorylation by the ATM kinase. In contrast, Thr98 is an integral element of the FHA structure. The crystal structure of the MDC1 FHA domain has not yet been solved, but a sequence comparison between the MDC1 FHA domain and the RAD53 FHA domain suggests that T98 is located within or near the β-sheet 7. This might be the reason why ATM is not able to phoshorylate Thr98, because the three dimensional structure allows no access for the kinase (see Figure 24).
FHA domains are phosphopeptide-binding domains with high specificity for phosphorylated threonines. Therefore, it is possible that Thr4 potentially interacts with such phosphopeptide-binding modules after it has been targeted by ATM in

response to DNA damage. No proteins have yet been identified that interact with the phosphorylated MDC1 N-terminal region. As MDC1 also contains an FHA domain, it is conceivable that MDC1 may form a homodimer in which each FHA domain binds to an opponent phospho-Thr4. Such a mode of interaction is currently object of investigations in our lab.

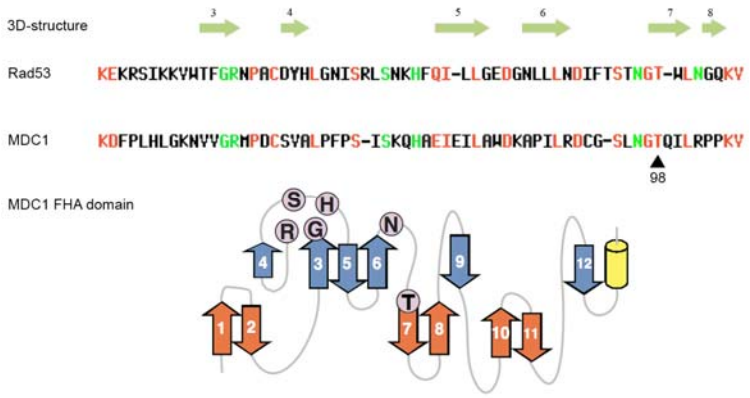

Figure 24; is a schematic illustration about conserved residues within FHA domains
Sequence comparisons of the MDC1 and the RAD53 FHA domains suggest that T98 is located within or near the β-sheet 7 and can consequently not be phosphorylated by ATM because the three dimensional structure allows ATM no access.

6.2. Development of a tandem affinity purification system for FHA and BRCT domains

In order to identify novel components of the DDR we decided to develop a Tandem affinity purification (TAP) system for FHA and BRCT domains. Many proteins in the DDR feature FHA or BRCT domains that interact with other proteins in a phosphorylation-dependent manner. It is published that BRCA1 interacts with phosphorylated BACH1, CtIP and Rap80 through its BRCT domain (see introduction). So we started this project using the BRCA1 BRCT domain in order to test if we can retrieve any of these proteins by our "*in vivo*" pull down strategy. The fusion protein, consisting of an EYFP, BRCA1 BRCT domains and the tag triplet, was stably expressed in U2OS cells. To test functionality of each tag, we first tested each tag individually by single-step pull downs.

In order to preserve proteins and prevent premature degradation we were using NTEN buffer consistent of EDTA, NaF, β-glycerol-phosphate and PMSF. EDTA inhibits

metalloproteases by forming complexes with metal ions, which are required in the catalytic subunit of these enzymes. PMSF is a serine protease inhibitor and NaF stops glycolysis by inhibiting the enzyme enolase. β-glycerol-phosphate is a phosphatase inhibitor. Additionally, NTEN buffer contains Nonidet P40 (NP40) a common nonionic detergent, used in many extraction protocols to solubilize membranes, especially nuclear membranes.

Analysis of the S-and Flag-tag pull-downs by immunoblot revealed strong binding of the recombinant fusion protein to the affinity matrices. However, analysis of the Strep-tag II pull-downs showed no or only very weak binding to the Streptavidin beads. This indicates that even though the fusion protein is expressed, the first step of the TAP is highly inefficient, thus impeding the entire TAP procedure.

When we designed our tag triplet, we had to choose between many different published peptide sequences that are binding to Streptavidin. To keep the tag as small as possible in order to avoid folding problems and to prevent any unspecific interactions with the rest of the protein, we have chosen the shortest tag available, the eight amino acid-long strep-tag II. Since the fusion protein didn't bind to the affinity matrix efficiently, we concluded that the strep-tag II is not ideally suited for our purpose. Indeed, strep-tag II has a higher affinity to streptactin, which is a genetically modified Streptavidin with increased affinity to Strep-tag I and Strep-tag II (Voss et. al. 1997). Because of the close relations between streptactin and Streptavidin we would have expected much stronger binding. It can be excluded that the fusion protein is not expressed as it still appears in the cell extract. However, it may be that the expression of the fusion protein was not efficient enough, so that the affinity between Strep-tag II and Streptavidin was too low to enrich it in the eluate fraction. Interestingly though, we did detect a band in the eluate at the size around 70kDa. It is rather unlikely that this band corresponds to our fusion protein, because the MW of the protein is too high. In addition, pull downs with Flag and S-tag resins revealed the fusion protein in the eluate at the same position as in the cell extract, indicating that the fusion protein does not shift in the gel upon binding to an affinity matrix. A closer look at the cell extract revealed a weak band at the size around 70kDa. We suggest that this protein somehow unspecifically interacts with Streptavidin and thereby accumulates in the eluate. Unfortunately, this protein does not only seem to bind to

Streptavidin, but it also seems to cross-react with the monoclonal α-Flag M2 antibody because otherwise it would not become visible on the anti-Flag immonoblot.

Even though we could readily detect the expression of the EYFP-BCRA1-BRCT fusion protein by Western Blot, we were not able to identify a prominent band representing the fusion protein in the silver stained SDS gels of the eluate fractions. This indicates that the fusion protein is only weakly expressed. Nevertheless, numerous bands are present in the eluate, most probably representing unspecific binding of proteins from the cell extracts to components of the affinity matrix. Detection of the fusion protein in the immunoblot may be a consequence of the high sensitivity of the antibodies. The Western Blot analysis of a Flag-tag pull down using a GFP-antibody showed a very strong signal in the eluate, which is another strong indication that the fusion protein is indeed enriched in the eluate by the M2 beads. However, this strong signal should not be over-interpreted, as the primary anti GFP antibody in this experiment was only diluted 1:1000, whereas recommendations from the manufacturer propose dilutions between 1:1000 and 1:5000. The low recombinant protein expression level of the stably transfected U2OS cells may be the result of the selection procedure and several passages of the stable clones before the experiments were carried out. We also detected low to average expression levels by fluorescence microscopy. In contrast, transiently transfected cells showed higher expression levels under the fluorescence microscope even though in this case, only a fraction of the cell population expressed the fusion protein. Unfortunately, pull-down assays from transiently transfected cells were also not successful (data not shown). In summary, a key criteria to achieve readily detectable fusion proteins in pull down eluates seems to be stable cell lines with high expression levels of the recombinant fusion protein. Since our fusion protein comprises an EYFP tag, fluorescence-activated cell sorting (FACS) may be applied to specifically select cells with high expression levels.

As described in the goals we originally planed to test if we could identify known interaction partners of the BRCA1 BRCT domains such as BACH1 or CtIP. However, since the first TAP step was highly inefficient, we were unable to achieve this goal within the given time frame. For the same reason we did not perform any pull down assays using the K1702M mutant.

For TAP, an efficient first purifiation step is absolutely vital. So the next step in this project will be to improve the fusion construct and gear it with another streptavidin binding tag. A Literature search revealed the 9 amino acids long Nano-tag (9) as a

promising new candidate for a Strep-binding partner. The Nano-tag (9) binds to streptavidin with a dissociation constant of 17nM (Lamla et. al. 2004). Other streptavidin binding tags show similar dissociation constants (Schmidt et. al., 1993), (Schmidt et.al. 1996), (Keefe et.al., 2001). In conclusion, to achieve the goal to find new interaction partners involved in the DDR we must improve our TAP system as we could show that the affinity between Strep-tag II and streptavidin was too low. A potential candidate is the Nano-tag (9). Pull down assays using the Flag- or S-tag revealed efficient binding and thus, don't need to be replaced. However, a further key issue is the low expression level disclosed by silver stained SDS gels from Flag- and S-tag pull downs. In order to increase the signal derived from the fusion protein versus background information we have to raise the expression level of the stably transfected cells. An improved selection process that specifically sorts out cells with high expression levels will hopefully bring success.

7. Abbreviations

α	Anti
aa	Amino acids
APS	Ammoniumperoxydisulfat
ATM	Ataxia Telangiectasia Mutated
ATP	Adenosine Triphoshpate
ATR	ATM Related
BACH1	BRCA1 Associated Carboxy-terminal Helicase 1 (syn. to BRIP or FancJ)
BARD1	BRCA1 associated RING domain 1
bp	Base pairs
BRCA1	Breast Cancer susceptibility protein 1
BRCT	BRCA1 Associated Carboxy-Terminus
BSA	Bovine Serum Albumine
Cdc25	Cell-division cycle 25
CdK	Cycline Dependent Kinase
CHK	Checkpoint Kinase
CIP	Calf Intestine Phosphatase
Crb2	Crumbs Homolog 2
CTBP	C-terminal Binding Protein
CtIP	CTBP interacting Protein
DAPI	4,6-Diamidino-2-phenylindol
DDR	DNA Damage Response
DTT	Dithiotritol
DNA	Desoxyribonucleic Acid
DNA-PK	DNA Dependent Kinase
DNA-PKcs	DNA-PK catalytic subunit
dNTP	Deoxynucleotide
ds	Double Stranded
DSB	DNA Double-strand Break
ECL	Enhanced Chemiluminescence
E.coli	Escherichia Coli
Ect2	Epithelial Cell Transforming Sequence 2
EDTA	Ethylendimin-tetraacetic Acid
EYFP	Enhanced Yellow Fluorescent Protein
FCS	Fetal Calf Serum
FHA	Forkhead Associated
γ	Phosphorylated
GFP	Green Fluorescent Protein

GSH	Glutathion
GST	Glutathion S-Transferase
H2AX	Histone 2A variant
HEPES	4-(Hydrosyethyl) Piperazine-1-ethanesulonic Acid
HNE	HeLa Nuclear Extract
HR	Homologous Recombination
IPTG	Isopropyl-β-thiogalactopyranoside
IR	Ionizing Radiation
IRIF	IR Induced Foci
kDa	Kilo Dalton
LB-medium	Luria-Bertani-medium
Lig 4	Ligase 4
MDC1	Mediator of DNA Damage Checkpoint 1
MRE11	Meiotic Recombination 11
MRN-complex	MRE11-RAD50-NBS1-complex
NBS1	Nijmegen Breakage Syndrome 1
NHEJ	Non-Homologues End Joining
NLS	Nuclear Localization Signal
NP40	Nonidet P40
OD	Optical Density
p53BP1	p53 Binding Protein 1
PARP	Poly (ADP-Ribose) Polymerase
PCR	Polymerase Chain Reaction
PIKK	Phosphatidylinositol 3-kinase like kinases
PMSF	Phenylmethansulfonylfluorid
PBS	Phosphate Buffered Saline
PNK	Polynucleotide Kinase
RAD50	RADiation sensitive yeast 50
RAP80	Receptor Associated Protein 80
RNA	Ribonucleic Acid
RNF8	Ring Finger Protein 8
ROS	Reactive Oxygen Species
rpm	Rounds Per Minute
ss	Single Stranded
SDS-PAGE	Sodium Dodecyl Sulfate – Polyacrylamid Electrophoresis
SER	Serine
UBC13	Ubiquitin-Conjugating Enzyme 13
TAP	Tandem Affinity Purification
TBST	Tris-Buffered Saline Tween-20
TEMED	N,N,N’,N’-Tetramethylethylendiamin

Tris	Tris-(hydrosymethyl)-aminomethan
UV	Ultraviloet
XRCC4	X-ray repair complementing defective repair in Chinese hamster cells 4

Amino acids:

Ala	A	Alanine
Gln	Q	Glutamine
Lys	K	Lysine
Met	M	Methionine
Ser	S	Serine
Thr	T	Threonine

8.1. References

Baer, R. and T. Ludwig (2002). "The BRCA1/BARD1 heterodimer, a tumor suppressor complex with ubiquitin E3 ligase activity." Curr Opin Genet Dev 12(1): 86-91.

Bakkenist, C. J. and M. B. Kastan (2003). "DNA damage activates ATM through intermolecular autophosphorylation and dimer dissociation." Nature 421(6922): 499-506.

Billack, B. and A. N. Monteiro (2004). "Methods to classify BRCA1 variants of uncertain clinical significance: the more the merrier." Cancer Biol Ther 3(5): 458-9.

Billack, B. and A. N. Monteiro (2005). "BRCA1 in breast and ovarian cancer predisposition." Cancer Lett 227(1): 1-7.

Bork, P., K. Hofmann, et al. (1997). "A superfamily of conserved domains in DNA damage-responsive cell cycle checkpoint proteins." FASEB J 11(1): 68-76.

Budman, J. and G. Chu (2005). "Processing of DNA for nonhomologous end-joining by cell-free extract." EMBO J 24(4): 849-60.

Callebaut, I. and J. P. Mornon (1997). "From BRCA1 to RAP1: a widespread BRCT module closely associated with DNA repair." FEBS Lett 400(1): 25-30.

Cantor, S. B., D. W. Bell, et al. (2001). "BACH1, a novel helicase-like protein, interacts directly with BRCA1 and contributes to its DNA repair function." Cell 105(1): 149-60.

Chapman, J. R. and S. P. Jackson (2008). "Phospho-dependent interactions between NBS1 and MDC1 mediate chromatin retention of the MRN complex at sites of DNA damage." EMBO Rep 9(8): 795-801.

Chen, A., F. E. Kleiman, et al. (2002). "Autoubiquitination of the BRCA1*BARD1 RING ubiquitin ligase." J Biol Chem 277(24): 22085-92.

Clapperton, J. A., I. A. Manke, et al. (2004). "Structure and mechanism of BRCA1 BRCT domain recognition of phosphorylated BACH1 with implications for cancer." Nat Struct Mol Biol 11(6): 512-8.

Costanzo, V., T. Paull, et al. (2004). "Mre11 assembles linear DNA fragments into DNA damage signaling complexes." PLoS Biol 2(5): E110.

Cromie, G. A., J. C. Connelly, et al. (2001). "Recombination at double-strand breaks and DNA ends: conserved mechanisms from phage to humans." Mol Cell 8(6): 1163-74.

D'Amours, D. and S. P. Jackson (2002). "The Mre11 complex: at the crossroads of dna repair and checkpoint signalling." Nat Rev Mol Cell Biol 3(5): 317-27.

Durocher, D. and S. P. Jackson (2002). "The FHA domain." FEBS Lett 513(1): 58-66.

Durocher, D., S. J. Smerdon, et al. (2000). "The FHA domain in DNA repair and checkpoint signaling." Cold Spring Harb Symp Quant Biol 65: 423-31.

Durocher, D., I. A. Taylor, et al. (2000). "The molecular basis of FHA domain:phosphopeptide binding specificity and implications for phospho-dependent signaling mechanisms." Mol Cell 6(5): 1169-82.

Falck, J., J. Coates, et al. (2005). "Conserved modes of recruitment of ATM, ATR and DNA-PKcs to sites of DNA damage." Nature 434(7033): 605-11.

Grawunder, U., D. Zimmer, et al. (1998). "DNA ligase IV is essential for V(D)J recombination and DNA double-strand break repair in human precursor lymphocytes." Mol Cell 2(4): 477-84.

Hammarsten, O., L. G. DeFazio, et al. (2000). "Activation of DNA-dependent protein kinase by single-stranded DNA ends." J Biol Chem 275(3): 1541-50.

Harper, J. W. and S. J. Elledge (2007). "The DNA damage response: ten years after." Mol Cell 28(5): 739-45.

Hartley, K. O., D. Gell, et al. (1995). "DNA-dependent protein kinase catalytic subunit: a relative of phosphatidylinositol 3-kinase and the ataxia telangiectasia gene product." Cell 82(5): 849-56.

Hemminki, K., X. Li, et al. (2004). "Familial risk of cancer: data for clinical counseling and cancer genetics." Int J Cancer 108(1): 109-14.

Hoeijmakers, J. H. J. (2001). "Genome maintenance mechanisms for preventing cancer." nature.

Hofmann, K. and P. Bucher (1995). "The FHA domain: a putative nuclear signalling domain found in protein kinases and transcription factors." Trends Biochem Sci 20(9): 347-9.

Huen, M. S., R. Grant, et al. (2007). "RNF8 transduces the DNA-damage signal via histone ubiquitylation and checkpoint protein assembly." Cell 131(5): 901-14.

Jackson, S. P. (2002). "Sensing and repairing DNA double-strand breaks." Carcinogenesis 23(5): 687-96.

Jazayeri, A., J. Falck, et al. (2006). "ATM- and cell cycle-dependent regulation of ATR in response to DNA double-strand breaks." Nat Cell Biol 8(1): 37-45.

Keefe, A. D., D. S. Wilson, et al. (2001). "One-step purification of recombinant proteins using a nanomolar-affinity streptavidin-binding peptide, the SBP-Tag." Protein Expr Purif 23(3): 440-6.

Khanna, K. K. and S. P. Jackson (2001). "DNA double-strand breaks: signaling, repair and the cancer connection." Nat Genet 27(3): 247-54.

Kobayashi, J., H. Tauchi, et al. (2002). "NBS1 localizes to gamma-H2AX foci through interaction with the FHA/BRCT domain." Curr Biol 12(21): 1846-51.

Koonin, E. V., S. F. Altschul, et al. (1996). "BRCA1 protein products ... Functional motifs." Nat Genet 13(3): 266-8.

Lamla, T. and V. A. Erdmann (2004). "The Nano-tag, a streptavidin-binding peptide for the purification and detection of recombinant proteins." Protein Expr Purif 33(1): 39-47.

Liang, X. and S. R. Van Doren (2008). "Mechanistic insights into phosphoprotein-binding FHA domains." Acc Chem Res 41(8): 991-9.

Lou, Z., B. P. Chen, et al. (2004). "MDC1 regulates DNA-PK autophosphorylation in response to DNA damage." J Biol Chem 279(45): 46359-62.

Lou, Z., K. Minter-Dykhouse, et al. (2003). "MDC1 is coupled to activated CHK2 in mammalian DNA damage response pathways." Nature 421(6926): 957-61.

Ma, Y., U. Pannicke, et al. (2002). "Hairpin opening and overhang processing by an Artemis/DNA-dependent protein kinase complex in nonhomologous end joining and V(D)J recombination." Cell 108(6): 781-94.

Mailand, N., S. Bekker-Jensen, et al. (2007). "RNF8 ubiquitylates histones at DNA double-strand breaks and promotes assembly of repair proteins." Cell 131(5): 887-900.

Manke, I. A., D. M. Lowery, et al. (2003). "BRCT repeats as phosphopeptide-binding modules involved in protein targeting." Science 302(5645): 636-9.

Martensson, S. and O. Hammarsten (2002). "DNA-dependent protein kinase catalytic subunit. Structural requirements for kinase activation by DNA ends." J Biol Chem 277(4): 3020-9.

Monteiro, A. N., A. August, et al. (1996). "Evidence for a transcriptional activation function of BRCA1 C-terminal region." Proc Natl Acad Sci U S A 93(24): 13595-9.

Paz-Elizur, T., R. Ben-Yosef, et al. (2006). "Reduced repair of the oxidative 8-oxoguanine DNA damage and risk of head and neck cancer." Cancer Res 66(24): 11683-9.

Riha, K., M. L. Heacock, et al. (2006). "The role of the nonhomologous end-joining DNA double-strand break repair pathway in telomere biology." Annu Rev Genet 40: 237-77.

Schmidt, T. G., J. Koepke, et al. (1996). "Molecular interaction between the Strep-tag affinity peptide and its cognate target, streptavidin." J Mol Biol 255(5): 753-66.

Schmidt, T. G. and A. Skerra (1993). "The random peptide library-assisted engineering of a C-terminal affinity peptide, useful for the detection and purification of a functional Ig Fv fragment." Protein Eng 6(1): 109-22.

Schmidt, T. G. and A. Skerra (2007). "The Strep-tag system for one-step purification and high-affinity detection or capturing of proteins." Nat Protoc 2(6): 1528-35.

Scully, R., A. Xie, et al. (2004). "Molecular functions of BRCA1 in the DNA damage response." Cancer Biol Ther 3(6): 521-7.

Shrivastav, M., L. P. De Haro, et al. (2008). "Regulation of DNA double-strand break repair pathway choice." Cell Res 18(1): 134-47.

Smith, G. C., N. Divecha, et al. (1999). "DNA-dependent protein kinase and related proteins." Biochem Soc Symp 64: 91-104.

Smolka, M. B., S. H. Chen, et al. (2006). "An FHA domain-mediated protein interaction network of Rad53 reveals its role in polarized cell growth." J Cell Biol 175(5): 743-53.

Sobhian, B., G. Shao, et al. (2007). "RAP80 targets BRCA1 to specific ubiquitin structures at DNA damage sites." Science 316(5828): 1198-202.

Spycher, C., E. S. Miller, et al. (2008). "Constitutive phosphorylation of MDC1 physically links the MRE11-RAD50-NBS1 complex to damaged chromatin." J Cell Biol 181(2): 227-40.

Stewart, G. S., B. Wang, et al. (2003). "MDC1 is a mediator of the mammalian DNA damage checkpoint." Nature 421(6926): 961-6.

Stucki, M., J. A. Clapperton, et al. (2005). "MDC1 directly binds phosphorylated histone H2AX to regulate cellular responses to DNA double-strand breaks." Cell 123(7): 1213-26.

Stucki, M. and S. P. Jackson (2004). "Tudor domains track down DNA breaks." Nat Cell Biol 6(12): 1150-2.

Stucki, M. and S. P. Jackson (2006). "gammaH2AX and MDC1: anchoring the DNA-damage-response machinery to broken chromosomes." DNA Repair (Amst) 5(5): 534-43.

Vandenberg, C. J., F. Gergely, et al. (2003). "BRCA1-independent ubiquitination of FANCD2." Mol Cell 12(1): 247-54.

Vogelstein, B. (2004). "Cancer genes and the pathways they control." Nature medicine.

Voss, S. and A. Skerra (1997). "Mutagenesis of a flexible loop in streptavidin leads to higher affinity for the Strep-tag II peptide and improved performance in recombinant protein purification." Protein Eng 10(8): 975-82.

Wang, B. and S. J. Elledge (2007). "Ubc13/Rnf8 ubiquitin ligases control foci formation of the Rap80/Abraxas/Brca1/Brcc36 complex in response to DNA damage." Proc Natl Acad Sci U S A 104(52): 20759-63.

Yu, X., C. C. Chini, et al. (2003). "The BRCT domain is a phospho-protein binding domain." Science 302(5645): 639-42.

Yu, X., L. C. Wu, et al. (1998). "The C-terminal (BRCT) domains of BRCA1 interact in vivo with CtIP, a protein implicated in the CtBP pathway of transcriptional repression." J Biol Chem 273(39): 25388-92.

Zhang, X., S. Morera, et al. (1998). "Structure of an XRCC1 BRCT domain: a new protein-protein interaction module." EMBO J 17(21): 6404-11.

Zhou, B. B. and S. J. Elledge (2000). "The DNA damage response: putting checkpoints in perspective." Nature 408(6811): 433-9.

8.2. List of Figures

Figure 1; Budman, J. and G. Chu (2005). "Processing of DNA for nonhomologous end-joining by cell-free extract." EMBO J 24(4): 849-60.

Figure 2; Zhou, B. B. and S. J. Elledge (2000). "The DNA damage response: putting checkpoints in perspective." Nature 408(6811): 433-9.

Figure 5; Durocher, D. and S. P. Jackson (2002). "The FHA domain." FEBS Lett 513(1): 58-66.

Figure 6; Zhang, X., S. Morera, et al. (1998). "Structure of an XRCC1 BRCT domain: a new protein-protein interaction module." EMBO J 17(21): 6404-11.

9. Appendix

9.1. Buffers, Medias and Solutions

Blue Dye	1ml Bromphenol blue 0.5ml β-mercapto-ethanol (14.2M) add dH2O to 10ml
Buffer D	2ml Hepes (1M) 3.33ml KCl (3M) 23ml Glycerol (87%) 40µl EDTA (0.5M) add dH2O to 100ml add 0.5µl DTT (1M) to 1ml buffer before use
Buffer E	100µl HEPES (0.5) 30µl NaCl (5M) 2µl EDTA (0.5M) 50µl NP40 (10%) 10µl PMSF (100mM) 1µl Leupeptin (1mg/ml) 1µl Pepstatin (1mg/ml) 1µl Bestatin (1mg/ml) add dH2O to 1ml
CaCl2 solution (2M)	2.22g CaCl2 in 10ml dH2O
Destain	400ml MetOH 10ml Acetic Acid add dH2O to 1000ml
Developing solution	3g NaCO3 50µl HCHO in 100ml H2O

Dialysis buffer	100ml 10xTBS 115ml 87% Glycerol add dH2O to 1000ml
E1A lysis buffer	10ml ELB 100µl EDTA (0.5M) 10µl DTT (1M) 100µl PMSF (100mM)
ELB buffer	25ml Tris (1M) 15ml NaCl (5M) 25ml NP40 (10%) add dH2O to 500ml
Extraction buffer	1.2ml Tris (1M, pH 6.8) 2.3ml Glycerol (87%) 2ml SDS (20%) add dH2O to 10ml
10x HBS	5g Hepes 8g NaCl 0.37g KCl 1g Dextrose 0.103g NaHPO4 add dH2O to 100ml
IP buffer	3.33ml KCl (3M) 1ml Hepes (1M) 4.6ml Glycerol (87%) 80µl MgCl2 (1M) 40µl EDTA (0.5M) 0.4ml NaF (100mM) 0.4ml β-glycerol-phosphat (100mM) 0.4ml NP40 (10%) add dH2O to 40ml

Kinase buffer	1ml Hepes (1M) 0.6ml NaCl (5M) 80µl MnCl2 (1M) 120µl MgCl2 (1M) 2.3ml Glycerol (87%) 20µl DTT (1M) 0.2ml NaF (100mM) 0.2ml β-glycerol-phosphat (100mM) add dH2O to 20ml
LB medium (Luria-Bertani medium)	10g Bactotryptone 5g Bacto-yeast extract 10g NaCl in 1l dH2O adjust pH to 7.0 with NaOH
6x Loading buffer	30ml Glycerol (87%) 0.5g Bromphenol blue 0.5g Xylen Cynol add dH2O to 200ml
NTEN buffer	7.5ml NaCl (5M) 5ml Tris (1M, pH 7.5) 0.5ml EDTA (0.5M) 12.5ml NP40 (10% solution) add dH2O to 250ml add just before use 2.5ml NaF (0.1M) 2.5ml β-glycerol-phosphat (1M) 1.25ml PMSF (0.2M)
1kb Marker	30µl 1kb Marker 6x loading buffer add dH2O to 100µl

PBS (Phosphat-buffered saline)	8g NaCl 0.2g KCl 1.44g Na2HPO 0.24g KH2PO add dH2O to 1l adjust pH to 7.4 with HCl
Ponceau S	2g Ponceau S 30g Trichloridacid 30g Sulfatsalicyl acid add dH2O to 100ml
2x Running-gel buffer	150ml Tris (1M, pH 8.8) 2ml SDS (20%) add dH2O to 200ml
10x Running buffer	60.6g Tris 288.2g Glycin add dH2O to 2l
20% SDS	40g SDS add dH2O to 200ml
2x SDS loading buffer	1ml Tris (1M, pH 6.8) 50µl β-mercapto ethanol 2ml SDS (20%) 200µl Bromphenol blue 2ml Glycerol (87%)
Silver solution	0.1g AgNO3 in 100ml dH2O
SOB	20g Bacto-Trypton 5g Bacto-yeast extract 0.5g NaCl add dH2O to 1000ml 10ml KCl (250mM) adjust pH to 7.0 with NaOH 5ml MgCl2 (5M) just before use

SOB++	1l SOB 10ml $MgSO_4$ just before use
SOC	980ml SOB 20ml Glucose (1M)
Solution A	5g Na_2CO_3 1g NaOH add dH_2O to 250ml
Solution B	50mg $CuSO_4(5H_2O)$ 0.1g Sodium citrate add dH_2O to 10ml
Stacking-gel buffer	30.2ml Tris (1M, pH6.8) 1.2ml SDS (20%) 100µl Bromphenol blue add dH_2O to 200ml
Stain	0.25g Coomassie Brilliant Blue R250 100ml MeOH 25ml Acetic acid add dH_2O to 250ml
Stripping buffer	1.25ml Tris (1M, pH 6.8) 1.6ml SDS (20%) 140µl β-mercapto-ethanol add dH_2O to 20ml
1x TAE buffer	4.84g Tris 1.14g Gluacal acetic acid 2ml EDTA (0.5M, pH8) add dH_2O to 1000ml
TB buffer	5ml Hepes (0.5M, pH 6.7) 3.75ml $CaCl_2$ (1M) 25ml KCl (2.5M) add dH_2O to 250ml adjust pH to 6.7 with KOH add 27.5ml $MnCl_2$ (0.5M) before use

1x TBS buffer	12.1g Tris 87.7g NaCl add dH2O to 1000ml
TBS-T	1l TBS 0.5ml Tween 20
Transfer buffer	100ml Running buffer (10%) 200ml Methanol add dH2O to 1l

9.2. Primers and Oligonucleotides

53bp1_BRCT_for
5’-CGC GGA TCC TTG CCT CTC AAC AAG ACC-3’

53bp1_BRCT_rev
5’-CGC TCT AGA GTG AGA AAC ATA ATC GTG-3’

53bp1_BRCT_for_K1814M
5’-CAG CAT TGT CGA ACC CGG ATG TAC TTC CTG TGC CTT GCC-3’

53BP1_BRCT_rev_K1814M
5’-GGC AAG GCA CAG GAA GTA CAT CCG GGT TCG ACA ATG CTG-3’

BRCA1_BRCT_for
5’-CGC GGA TCC GAA AGG GTC AAC AAA AGA A-3’

BRCA1_BRCT_rev
5’-GCT CTA GAT CAG TAG TGG CTG TGG GGG-3’

BRCA1_rev_noStop
5’-GCT CTA GAG TAG TGG CTG TGG GGG ATC TGG-3’

for_K1702M_BRCA1
5’-GTG TGT GAA CGG ACA CTG ATG TAT TTT CTA GGA ATT GCG G-3’

rev_K1702M_BRCA1
5’-CCG CAA TTC CTA GAA AAT ACA TCA GTG TCC GTT CAC ACA C-3’

for_Tags_03.12.08
5’-GAT CCG CGT CTA GAA AAG AAA CCG CTG CTG CGA AAT TTG AAC GCC AGC ACA TGG ACT CGG CGG ACT ACA AAG ACG ATG ACG ACA AGG CGG ATG TTG AAG CTT GGC TTG ACG AAC GTG-3’

rev_Tags_03.12.08
5’-CTA GCA CGT TCG TCA AGC CAA GCT TCA ACA TCC GCC TTG TCG TCA TCG TCT TTG TAG TCC GCC GAG TCC ATG TGC TGG CGT TCA AAT TTC GCA GCA GCG GTT TCT TTT CTA GAC GCG-3’

M-1 T4A_fw
5’- CTG GAT CCA TGG AGG ACG CCC AGG CTA TTG ACT GGG ATG -3’

M_FHA_rev
5’- GCT CTA GAC TGT ACT CTG GGT GTC TCT TCT ACT G -3’

MDC1_BRCT_for
5’-CGC GGA TCC GCA GAG GAG GAG CCC AAC AG-3’

MDC1_BRCT_rev
5’-CGC TCT AGA GGT GGA TGA CAT CTC CAA AG-3’

S-Flag-Strep-for
5’-GAT CCG CGT CTA GAA AAG AAA CCG CTG CTG CGA AAT TTG AAC GCC AGC ACA TGG ACT CGG CGG ACT ACA AAG ACG ATG ACG ACA AGG CGT GGA GCC ACC CGC AGT TCG AAA AAG-3’

S-Flag-Strep-rev
5’-CTA GCT TTT TCG AAC TGC GGG TGG CTC CAC GCC TTG TCG TCA TCG TCT TTG TAG TCC GCC GAG TCC ATG TGC TGG CGT TCA AAT TTC GCA GCA GCG GTT TCT TTT CTA GAC GCG-3’

T4Agex-for
5’-GTG GAT CCA TGG AGG ACG CCC AGG CTA TTG ATCT GG-3’

T4Agex_rev
5’-CCA GTC AAT AGC CTG GGC GTC CTC CAT GGA TCC AC-3’

9.3 Sequencing Results

Sequence report of the T4A mutant N-terminal fragment of MDC1

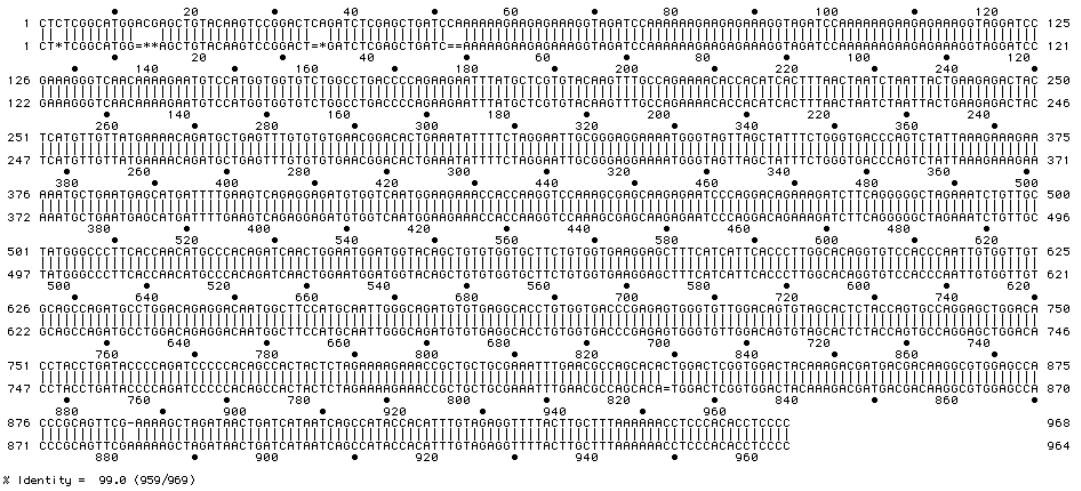

Sequence Report of the BRCA1 BRCT domain

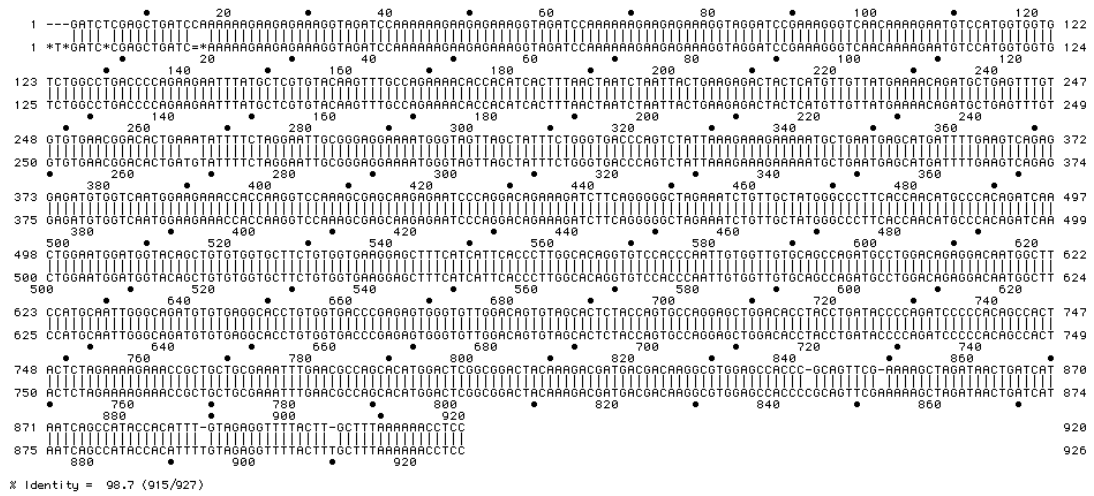

Sequence Report of the K1702M mutant BRCA1 BRCT domain

10. Acknowledgements

I would like to give a great thank to Dr. Manuel Stucki for being an excellent supervisor. His wide knowledge and the will to share it, combined with such didactic skills that even I could understand, helped me a lot.

Special gratitude to Prof. Dr. Michael Hottiger for his great commitment in organizing the major course in biomedical research.

And of course I am deeply indebted to all my colleagues of the IVBMB, especially to the director of the institute Prof. Dr. Ulrich Hübscher.

I would also like to give a big shut out to my fellaz from the Westside; Steffi and Luci and to my Homies from the Eastside; Flurina and Christoph. You will always stay in my mind as “die Gurkentruppe”. Thanx for everything and that you still talk to me. Keep the battle goin’ on!!!

I would like to express my deep and sincere gratitude to the DIC crew. The future will be ours!

I thank my Mämä and my Bäbä, you’re doing a great job…

And finally I would like to give special thanks (and kisses) to my girlfriend Sévi for loving and accepting me and all my other personalities!

“Not everything is as serious as it seems.”

Mario Bonalli alias die Obergurke

11. Lebenslauf

Name, Vorname	Bonalli Mario-Emanuel
Geburtsdatum	17.05.1983
Geburtsort	Zürich
Nationalität	Schweizer
Heimatort	Zürich
08/1990- 07/1996	Primarschule in Oberengstringen, Schweiz
08/1996- 07/1998	Sekundarschule in Oberengstringen, Schweiz
07/1998- 09/2002	Gymnasium an der Kantonsschule Limmattal in Urdorf, Schweiz
22/09/2002	Abschluss der Mathematisch-naturwissenschaftlichen Matur Schwerpunkt Biologie und Chemie
10/2004- 10/2009	Studium der Veterinärmedizin an der Universität Zürich, Schweiz
15/10/2009	Diplom der Veterinärmedizin an der Universität Zürich, Schweiz

Erstellt am 07.09.2009